Applying the Newmark Method into the Discontinuous Deformation Analysis

Bo Peng

Thesis submitted to the Faculty of the

Virginia Polytechnic Institute and State University

in partial fulfillment of the requirements for the degree of

Master of Science

in

Computer Science and Applications

Yang Cao

Linbing Wang

Alexey Onufriev

September 15, 2014

Blacksburg, Virginia

Keywords: Newmark method, Discontinuous deformation analysis, Rock mechanics

Applying the Newmark Method into the Discontinuous Deformation Analysis

Bo Peng

(ABSTRACT)

Discontinuous deformation analysis (DDA) is a newly developed simulation method for discontinuous systems. It was designed to simulate systems with arbitrary shaped blocks with high efficiency while providing accurate solutions for energy dissipation. But DDA usually exhibits damping effects that are inconsistent with theoretical solutions. The deep reason for these artificial damping effects has been an open question, and it is hypothesized that these damping effects could result from the time integration scheme. In this thesis two time integration methods are investigated: the forward Euler method and the Newmark method.

The work begins by combining the Newmark method and the DDA. An integrated Newmark method is also developed, where velocity and acceleration do not need to be updated. In simulations, two of the most widely used models are adopted to test the forward Euler method and the Newmark method. The first one is a sliding model, in which both the forward Euler method and the Newmark method give accurate solutions compared with analytical results. The second model is an impacting model, in which the Newmark method has much better accuracy than the forward Euler method, and there are minimal damping effects.

Dedication

This thesis is dedicated to my parents: Xiaochu Peng and Hongbo Tang,

Acknowledgments

I would like to give my sincere gratitude to Dr. Yang Cao, who is an incredible advisor: taught me the attitude to the research, trained me professionally, revised my thesis three times and helped me rehearsal presentation three times. Besides, he is very caring and considerate, which helps me make through my second degree (CS) really smoothly. My appreciation goes to Dr. Linbing Wang in CEE department, who is my advisor in CEE department and my committee member in CS research. He provided me great opportunities to study and research in Virginia Tech. I would like to thank my committee member Dr. Alexey Onufriev. I cannot realize my limitation without his help and suggestion. I also want to thank my group mates: Fei Li, Shuo Wang, Minghan Chen. I enjoyed the friendship with you.

I want to thank my parents for their forever love and supports. I can achieve nothing without them. I am thankful for my roommates, my dance crew mates, and my very supportive friend Cris. They are the irreplaceable parts in my Blacksburg life.

Contents

List of Figures

Chapter 1

Introduction

Rock, as a widely existing material in nature, is closely related to our daily life: falling rocks near highway might result in serious accidents; slope stability is one of the key factors to ensure safety of construction activities on either man-made or natural slops. From irregular aggregates to huge rock mountains, rock systems are highly discrete. Therefore, it is very important to develop models and simulation methods to help us understand discrete rock systems.

There are several popular simulation methods to simulate the dynamic behavior of rock systems, such as the finite element method (FEM), the discontinuous deformation analysis (DDA) and the discrete element methods (DEM). In these three methods, the FEM is mainly used for continuous problems, while the DDA and the DEM are designed for discrete systems.

The finite element method (FEM) is a popular simulation method to simulate mechanical systems[5,6] . However, in terms of discontinuous materials, especially for blocky systems, the FEM is

highly restricted when solving big deformation problems, while discrete methods (e.g. DDA and DEM) do not have this shortcoming.

The discrete element method (DEM), first proposed by Cundall in 1979,[7] has been developed rapidly worldwide since then. The DEM can be applied in a wide range of research areas, including the particle fluidization of cohesionless and cohesive particle flow, confined or unconfined particle flow, particle flow in hoppers, in mixers, in drums and mills, particle packing, compaction of particles, etc. The advantage of the DEM is that it can simulate heterogeneity materials through discretization. Setting different parameters to the contributing materials in the simulation helps to distinguish their interaction. An example of the DEM asphalt binder simulation with irregular shaped aggregates is shown in Figure 1.1. In the simulation two different materials, aggregates and asphalt, were developed in the same specimen, and clumps of particles were used to simulate irregular shaped aggregates. Although DEM is design for discrete systems, it has defects such as inaccurate artificial energy dissipation estimation and not sophisticated contact interaction models. Therefore, the DEM is restricted in particle flow problems.

The discontinuous deformation analysis (DDA) was first proposed by Shi in 1988.[8] Because of its advantages such as high accuracy, reasonable contact interaction model, relatively low computational cost etc., the DDA shows great potential to be a powerful tool for simulating discrete rock systems. Besides the original two-dimensional DDA, some extended methods are developed, including the backward DDA,[9] the particle DDA,[10] the manifold method,[11] and the three dimensional DDA.[12] Validation results for DDA are obtained from comparison between DDA results and analytical solution, laboratory data, field data, and results of other discrete element analysis, such

as DEM. For validation with respect to analytical solution, works have been done on initiation of failure , rotation[13] , tensile strength,[13] sliding motion[14] and impacting behaviors.[15] For practical applications, the DDA has been applied to many engineering projects, such as the Three Gorges Dam in China,[16] Yerba Buena Tunnel in California,[17] Masada National Monument in Israel[18] and Pueblo Dam in Colorado.[19] An example for the DDA rocky system simulation is shown in Figure 1.2. Compared to clusters of particles in DEM, each irregular shaped block in DDA simulation is one object representing by surface and vertex information, as Figure 1.2 left shows. The right picture is a slope stability analysis for Bai He Tan Hydropower station using the DDA, and the highlighted red block is the most unstable rock. This example shows a great advantage of DDA: it can be used to solve problems in the real world directly, which is not achievable for the DEM so far.

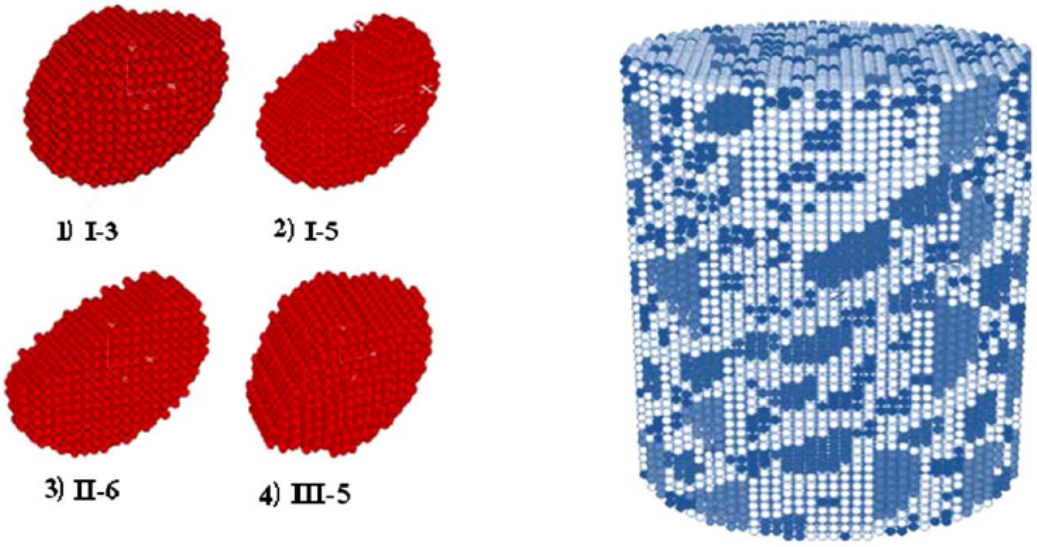

Figure 1.1: **Left:** Individual aggregates in DEM. **Right:** DEM simulation for aggregates in asphalt binder.

Y. Liu, *Discrete element methods for asphalt concrete: development and application of userdefined microstructural models and a viscoelastic micromechanical model*. Michigan Technological University, 2011. Used under fair use, 2014.

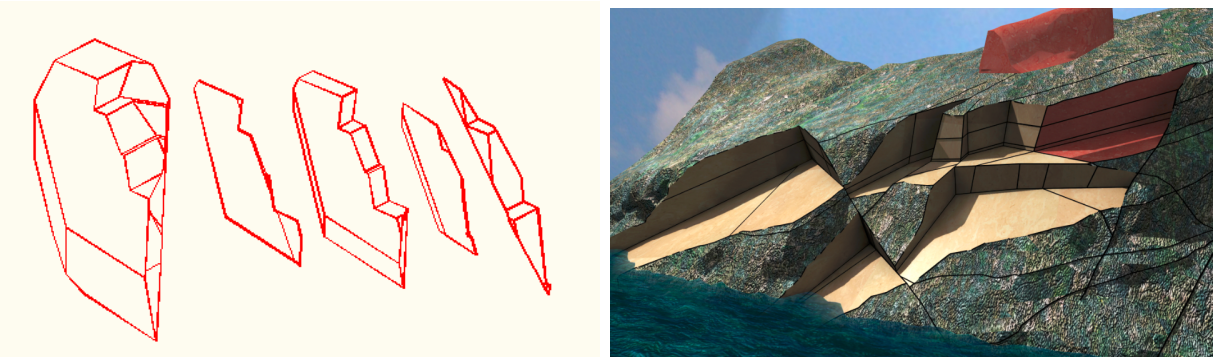

Figure 1.2: **Left:**irregular shaped blocks in the DDA simulation. **Right:** The DDA slope stability analysis for Bai He Tan Hydropower station.

X. Peng, *Stability reports for Baiheitan Dam*, 2003. Used under fair use, 2014.

1.1 Research Objects

The damping effects resulting from the DDA could be attributed as an inner defect. According to theoretical analysis,[20] there should be no energy dissipation under undamped situation. However, previous research[4,15,21] has shown an obvious damping effect in collision and oscillation simulations, and the damping effects increase when time-step size increases. Although efforts have been made to improve on this weakness, no effective/efficient remedy has been developed.

To overcome this shortcoming, we explored a new time integration method – the Newmark method,

and applied it to the DDA code. As mentioned above, the DDA is designed to simulate displacement changes with respect to time. For the velocity and acceleration information in the stiffness matrix, the global equation of the DDA can be formulated as a set of ordinary differential equations (ODEs). However, the swift changes of contact status cause the stiffness matrix in the ODEs to vary frequently. As a result, it is very inefficient to apply traditional ODE solvers to solve the global equation in the DDA. Therefore, highly discrete time integration methods must be applied to the DDA.

Prior to this work, only the forward Euler method was applied to DDA. In this thesis,the Newmark method is used as a time integration scheme in the DDA for the first time. A comprehensive comparison between the forward Euler method and the Newmark method when applied in the DDA will be studied based on two test models: a sliding model and an impacting model. These two models are the most basic testing models for the DDA method, because both models involve simulations of block contacting in both tangential and normal directions.

1.2 Organization

The main goal of research in this thesis is to improve the simulation accuracy of DDA through the Newmark method. The structure of this thesis is organized as following: Chapter two will give a brief description on the DDA theory and the research literature of DDA. Chapter three will introduce the application of the Newmark method in DDA, as well as an integrated Newmark method. Chapter four is going to illustrate the implement details, including the DDA code structure

and how to combine the Newmark method into DDA. Chapter five shows a comprehensive data analysis of the Newmark simulation. The results are compared to the traditional forward Euler simulation. Chapter six presents the conclusion of this thesis and proposes the future work to search for optimized parameters.

Chapter 2

Background

2.1 Introduction to the DDA

2.1.1 The Origin of the DDA

Before the description of the DDA, two basic rock definitions need to be introduced as below:

- Structure plane: there are geological surfaces with different factors and traits in rocks; such as joint, fracture, fault. Because of their existence, rock can not be considered as continuous material: rocks are split into irregular rock blocks. The interface separating rocks is called structure plane. Structure interfaces are with multiple scales of sizes and properties: some of them are big enough to present across the entire rock, while some others can not even be seen in the surface. With the tectonic movements for billions of years, there are a huge

amount of structure planes in rocks.

- Blocky system: intricate structure planes split rock mountain into many irregular rock blocks, which form blocky systems.

Because of the extreme anisotropy and its much lower strength than rock, structure plane is the place that material failure occurs most. The failure mode and movement mode vary tremendously with changes of structure planes.

With the understanding that structure planes play a key role in rock mechanics, the DDA considers each block as an individual object, and blocks interact with each other through contact forces. These properties of DDA simplify complicated blocky systems and their mechanical analysis, which make the simulation of complex blocky systems possible.

DDA Problem

Considering a practical engineering project: a tunnel is planed to be built across a rock mountain. Though the mountain is split by structure planes into large amount of individual rock blocks, it is stable before the tunnel is developed. However, a tunnel will change the structure stability of a mountain: rocks near the tunnel will lose some of their supports, and this will result in serious potential risks such as falling rocks. Therefore, it is very important to know how a tunnel influences the mountain stability. Figure 2.1 shows an example of tunnel stability analysis. Through DDA simulation, we know the information of unstable rocks, highlighted red block in picture, resulting from tunnel excavation. With these information, the tunnel can be stabilized through actions of

anchoring unstable rocks during construction.

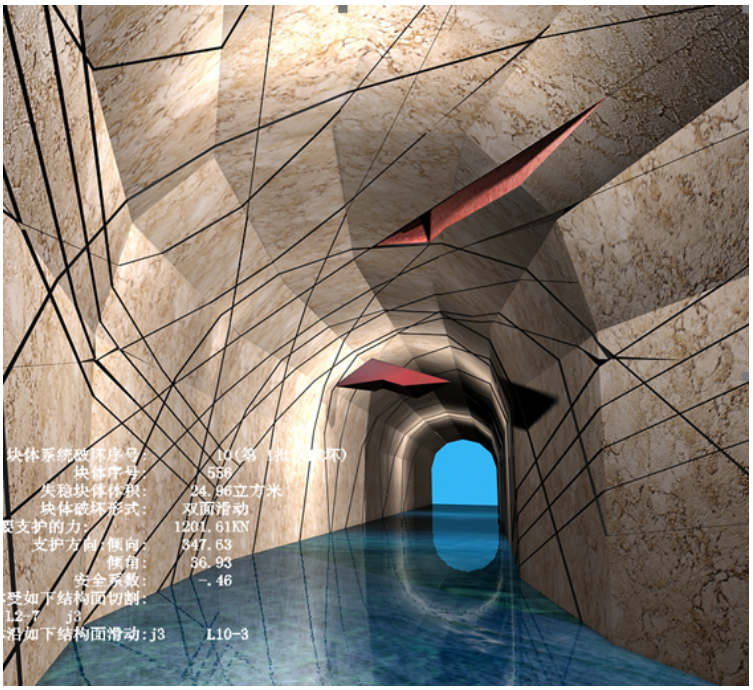

Figure 2.1: DDA simulation for unstable rocks in a tunnel

X. Peng, *Stability reports for Baiheitan Dam*, 2003. Used under fair use, 2014.

2.1.2 Time-step Loop

In order to simulate the movement and mechanical behavior of an object over a period of time, the DDA divides the entire process into many small time intervals and we call each interval one time-step. In every time-step the DDA solves a linear equilibrium equation, which takes the center displacement and rotation in each block as unknown variables. The linear equation is formulated with force equilibrium laws based on energy minimization principle: the forces in all directions are supposed to be balanced in every time-step. These forces include gravity, loading, inertial force and

other contacting forces. More details of equation formation in the DDA will be introduced in the next section. After solving the linear equation, we obtain the increment of displacement for each block in the current time-step. Then according to movement laws, the velocity and acceleration in the current step are acquired. Also, with the help of shape functions (relationship with center displacement and displacement of arbitrary points in the block), the coordinates of blocks' vertex can be obtained, as well as the positions of blocks. Based on those position information, the contact information will be determined. A time-step simulation is finished at this point, and this process will repeat until the simulation ends.

2.1.3 Interaction

In discrete blocky systems, blocks interact with each other through contacting. There are two types of contacting: vertex-plane contacts and edge-edge contacts. A contact is defined as the overlap between two blocks. After a contact is formed, the two blocks are considered as being connected with two springs: a normal spring and a tangential spring. The magnitude of spring forces is linear with the depth of the overlap, and the spring forces will be added to the linear equilibrium equation mentioned above.

2.1.4 Boundary Conditions

Boundary conditions in blocky systems are constrains. There are three different kinds of restrictions: rotation constrains, translation constrains and fixed constrains. The setting of boundary

conditions in the DDA is similar to that in the FEM: defining boundary conditions according to the system structure, and adding those information into the linear equilibrium equation.

2.1.5 Two Dimensional DDA and Three Dimensional DDA

When Dr. Shi proposed the DDA method for the first time, it was designed only for two-dimensional problems. For two dimensional DDA (2D-DDA),[8] there are only three basic unknown variables for each block: translation displacements in the X,Y directions and the rotation in the XY plane. After the three dimensional DDA (3D-DDA) was proposed in 2001,[12] the number of basic unknown variables extended to six: displacements in X,Y,Z directions and rotations in XY, YZ, XZ planes. With the 3D-DDA solution, it is possible to simulate all different types of movements. The unknown variables can also include the strain information as we will illustrate in the next.

2.2 Theoretical Three Dimensional DDA

This section is based on the 2D-DDA and 3D-DDA theoretical work done by Shi.[8,12]

2.2.1 The Complete First Order Approximation

Assume that a block, whose center is (x_0, y_0, z_0), has constant strain and stress. In the following we will demonstrate that the displacement (u, v, w) for an arbitrary point (x, y, z) in the block can

be denoted by twelve variables:

$$(u_0, v_0, w_0, r_1, r_2, r_3, \epsilon_x, \epsilon_y, \epsilon_z, \gamma_{xy}, \gamma_{yz}, \gamma_{xz}), \tag{2.1}$$

where u_0, v_0, w_0 are translation displacements for the center of the block, r_1, r_2, r_3 denote rotations, $\epsilon_x, \epsilon_y, \epsilon_z, \gamma_{xy}, \gamma_{yz}, \gamma_{xz}$ are normal and tangential strains for the block.

The complete first order approximation of displacements in a block can be denoted as:

$$\begin{aligned} u &= a_1 + a_2 x + a_3 y + a_4 z, \\ v &= b_1 + b_2 x + b_3 y + b_4 z, \\ w &= c_1 + c_2 x + c_3 y + c_4 z. \end{aligned} \tag{2.2}$$

The displacements on center of the block (x_0, y_0, z_0) can be denoted as:

$$\begin{aligned} u_0 &= a_1 + a_2 x_0 + a_3 y_0 + a_4 z_0, \\ v_0 &= b_1 + b_2 x_0 + b_3 y_0 + b_4 z_0, \\ w_0 &= c_1 + c_2 x_0 + c_3 y_0 + c_4 z_0. \end{aligned} \tag{2.3}$$

Then, subtracting Eq. (2.3) from Eq. (2.2):

$$\begin{aligned} u &= a_1 + a_2(x - x_0) + a_3(y - y_0) + a_4(z - z_0) + u_0, \\ v &= b_1 + b_2(x - x_0) + b_3(y - y_0) + b_4(z - z_0) + v_0, \\ w &= c_1 + c_2(x - x_0) + c_3(y - y_0) + c_4(z - z_0) + w_0. \end{aligned} \tag{2.4}$$

Considering the definitions of strain and rotation, we have

$$
\begin{aligned}
\epsilon_x &= \frac{\partial u}{\partial x} = a_2, \\
\epsilon_y &= \frac{\partial v}{\partial y} = b_3, \\
\epsilon_z &= \frac{\partial w}{\partial z} = c_4, \\
\frac{1}{2}\gamma_{xy} &= \frac{1}{2}(\frac{\partial v}{\partial x} + \frac{\partial u}{\partial y}) = \frac{1}{2}(b_2 + a_3), \\
\frac{1}{2}\gamma_{xz} &= \frac{1}{2}(\frac{\partial w}{\partial x} + \frac{\partial u}{\partial z}) = \frac{1}{2}(c_2 + a_4), \\
\frac{1}{2}\gamma_{yz} &= \frac{1}{2}(\frac{\partial w}{\partial y} + \frac{\partial v}{\partial z}) = \frac{1}{2}(c_3 + b_4), \\
r_1 &= \frac{1}{2}(\frac{\partial v}{\partial x} - \frac{\partial u}{\partial y}) = \frac{1}{2}(b_2 - a_3), \\
r_2 &= \frac{1}{2}(\frac{\partial w}{\partial x} - \frac{\partial u}{\partial z}) = \frac{1}{2}(c_2 - a_4), \\
r_3 &= \frac{1}{2}(\frac{\partial w}{\partial y} - \frac{\partial v}{\partial z}) = \frac{1}{2}(c_3 - b_4).
\end{aligned}
\tag{2.5}
$$

Rewrite Eq. (2.4) by using $(u_0, v_0, w_0, r_1, r_2, r_3, \epsilon_x, \epsilon_y, \epsilon_z, \gamma_{xy}, \gamma_{yz}, \gamma_{xz})$. We get a matrix format of

the complete first order equation for displacements:

$$\begin{pmatrix} u \\ v \\ w \end{pmatrix} = \begin{pmatrix} 1 & 0 & 0 \\ 0 & 1 & 0 \\ 0 & 0 & 1 \\ -(y-y_0) & (x-x_0) & 0 \\ 0 & -(z-z_0) & (y-y_0) \\ (z-z_0) & 0 & -(x-x_0) \\ (x-x_0) & 0 & 0 \\ 0 & (y-y_0) & 0 \\ 0 & 0 & (z-z_0) \\ (y-y_0)/2 & (x-x_0)/2 & 0 \\ 0 & (z-z_0)/2 & (y-y_0)/2 \\ (z-z_0)/2 & 0 & (x-x_0)/2 \end{pmatrix}^T \begin{pmatrix} u_0 \\ v_0 \\ w_0 \\ r_1 \\ r_2 \\ r_3 \\ \epsilon_x \\ \epsilon_y \\ \epsilon_z \\ \gamma_{xy} \\ \gamma_{yz} \\ \gamma_{xz} \end{pmatrix}. \tag{2.6}$$

For the block i, the displacement equation Eq. (2.6) can be rewritten as:

$$\begin{pmatrix} u \\ v \\ w \end{pmatrix} = [T_i]\{D_i\}. \tag{2.7}$$

A higher order approximation can be derived by increasing the dimension of $[T_i], \{D_i\}$.

2.2.2 Energy Minimization and Equilibrium Equation

Contacts between blocks and restrictions integrate blocks into a system. Assume there are n blocks, then the equilibrium equations for the system are given by

$$\begin{pmatrix} K_{11} & K_{12} & K_{13} & \cdots & K_{1n} \\ K_{21} & K_{22} & K_{23} & \cdots & K_{2n} \\ K_{31} & K_{32} & K_{33} & \cdots & K_{3n} \\ \vdots & \vdots & \vdots & \ddots & \vdots \\ K_{n1} & K_{n2} & K_{n3} & \cdots & K_{nn} \end{pmatrix} \begin{pmatrix} D_1 \\ D_2 \\ D_3 \\ \vdots \\ D_n \end{pmatrix} = \begin{pmatrix} F_1 \\ F_2 \\ F_3 \\ \vdots \\ F_n \end{pmatrix}. \tag{2.8}$$

There are twelve degrees of freedom $(u_0, v_0, w_0, r_1, r_2, r_3, \epsilon_x, \epsilon_y, \epsilon_z, \gamma_{xy}, \gamma_{yz}, \gamma_{xz})$ for each block, therefore, $\{D_i\}, \{F_i\}$ are both 12×1 vectors, and $[K_{ij}]$ is a 12×12 matrix. $\{D_i\}$ denotes the displacement and strain for each block in one time-step, $\{F_i\}$ saves the loading information, and $[K_{ii}]$ stores the information of material of ith block, $[K_{ij}]$ stores the contact information between block i and block j.

The equilibrium equations are derived from minimization of the total potential energy, which is a function of forces and stress in the system. The i-th row of Eq. (2.8) is composed of twelve linear equations:

$$\frac{\partial \prod}{\partial d_{ri}} = 0, \quad r = 1, ..., 12, \tag{2.9}$$

where $\prod$ denotes the energy of entire system, and d_{ri} is the displacement information for the ith

block. The partial derivatives

$$\frac{\partial^2 \prod}{\partial d_{ri} \partial d_{sj}}, \quad r, s = 1...12 \tag{2.10}$$

are coefficients for unknown variable d_{sj} in Eq. (2.9). Therefore, all terms of Eq. (2.9) form a 12×12 matrix, which is a coefficient for submatrix $[K_{ij}]$ in the global equation Eq. (2.8). Eq. (2.10) also shows the symmetry of the stiff matrix $[K]$. The partial derivatives

$$-\frac{\partial \prod(0)}{\partial d_{ri}}, \quad r = 1...12 \tag{2.11}$$

are free terms for Eq. (2.8), and they will shift to the right side of that equation. Eq. (2.11) is a 12×1 vector, which is the subvector $\{F_i\}$ in Eq. (2.8).

2.2.3 Structure of Stiffness Matrix and Right-side Vector

The total energy is a function of six components: strain energy, energy of the initial constant stresses, energy from the point loading force, energy from volume loading (e.g. gravity), dynamic energy and contacts between blocks. We will present the equations corresponding to each component below.

Stiffness Submatrix

The strain energy can be denoted as an integration of strain times stress over the entire block:

$$\Pi_e = \int\int\int 1/2(\epsilon_x\sigma_x + \epsilon_y\sigma_y + \epsilon_z\sigma_z + \gamma_{xy}\tau_{xy} + \gamma_{xz}\tau_{xz} + \gamma_{yz}\tau_{yz})dxdydz. \tag{2.12}$$

The strain-stress relationship in the i-th block is given by

$$\{\epsilon_i\} = [E_i]\{\sigma_i\}, \tag{2.13}$$

where

$$[E_i] = \frac{E}{2(1+\nu)(1-2\nu)} \begin{pmatrix} 2(1-\nu) & 2\nu & 2\nu & 0 & 0 & 0 \\ 2\nu & 2(1-\nu) & 2\nu & 0 & 0 & 0 \\ 2\nu & 2\nu & 2(1-\nu) & 0 & 0 & 0 \\ 0 & 0 & 0 & 1-2\nu & 0 & 0 \\ 0 & 0 & 0 & 0 & 1-2\nu & 0 \\ 0 & 0 & 0 & 0 & 0 & 1-2\nu \end{pmatrix}. \tag{2.14}$$

The strain energy Eq. (2.12) can be rewritten as

$$\Pi_e = 1/2\int\int\int \{D_i\}^T[E_i]\{D_i\}dxdydz = S/2\{D_i\}^T[E_i]\{D_i\}, \tag{2.15}$$

where S is the volume of the i-th block.

Based on Eq. (2.15), the submatrix of stiffness matrix is acquired through minimization of the strain energy $\prod_e$:

$$k_{rs} = \frac{\partial^2 \Pi_e}{\partial d_{ri} \partial d_{si}} = \frac{\partial^2}{\partial d_{ri} \partial d_{si}} (\{D_i\}^T [E_i] \{D_i\}), \quad r, s = 1...12, \tag{2.16}$$

where k_{rs} is a 12×12 submatrix added to $[K_{ii}]$ in the global stiffness matrix:

$$S[E_i] \rightarrow [K_{ii}]. \tag{2.17}$$

Subvector of Initial Stress

If the i-th block is under an initial stress$({\sigma_x}^0, {\sigma_y}^0, {\sigma_z}^0, {\tau_{xy}}^0, {\tau_{xz}}^0, {\tau_{yz}}^0)$, the respective energy of the entire block is given by

$$\begin{aligned} \Pi_\sigma &= \int\int\int 1/2(\epsilon_x {\sigma_x}^0 + \epsilon_y {\sigma_y}^0 + \epsilon_z {\sigma_z}^0 + \gamma_{xy} {\tau_{xy}}^0 + \gamma_{xz} {\tau_{xz}}^0 + \gamma_{yz} {\tau_{yz}}^0) dxdydz \\ &= -S(\epsilon_x {\sigma_x}^0 + \epsilon_y {\sigma_y}^0 + \epsilon_z {\sigma_z}^0 + \gamma_{xy} {\tau_{xy}}^0 + \gamma_{xz} {\tau_{xz}}^0 + \gamma_{yz} {\tau_{yz}}^0) \end{aligned} . \tag{2.18}$$

Let

$$[\sigma_0]^T = \left([\mathbf{0}]_{\mathbf{6 \times 1}} \quad {\sigma_x}^0 \quad {\sigma_y}^0 \quad {\sigma_z}^0 \quad {\tau_{xy}}^0 \quad {\tau_{xz}}^0 \quad {\tau_{yz}}^0 \right), \tag{2.19}$$

then rewrite Eq. (2.18) as

$$\Pi_\sigma = -S\{D_i\}^T \{\sigma_0\}. \tag{2.20}$$

Minimizing Π_σ by taking the derivatives:

$$f_r = -\frac{\partial \Pi_\sigma}{\partial d_{ri}} = S\frac{\partial \{D_i\}^T \{\sigma_0\}}{\partial d_{ri}} \quad r = 1...12, \tag{2.21}$$

where f_r is a 12×1 vector, and it will be added to the global force vector:

$$S\{\sigma_0\} \rightarrow \{F_i\}. \tag{2.22}$$

Subvector of Point Loading

The energy raised by a point load (F_x, F_y, F_z) at a point (x, y, z) can be denoted as:

$$\Pi_p = -(u\ v\ w) \begin{pmatrix} F_x \\ F_y \\ F_z \end{pmatrix} = -\{D_i\}^T [T_i(x, y, z)]^T \begin{pmatrix} F_x \\ F_y \\ F_z \end{pmatrix}. \tag{2.23}$$

After minimizing this part of energy, a 12×1 loading vector will be added to the global loading vector:

$$[T_i(x, y, z)]^T \begin{pmatrix} F_x \\ F_y \\ F_z \end{pmatrix} \rightarrow \{F_i\}. \tag{2.24}$$

Subvector of Volume Load

Assume that (f_x, f_y, f_z) is a volume load applied on the ith block, then the potential energy from the volume load is:

$$\Pi_s = -\int\int\int (u\ v\ w) \begin{pmatrix} f_x \\ f_y \\ f_z \end{pmatrix} dx\ dy\ dz = -\{D_i\}^T \int\int\int [T_i]^T dx\ dy\ dz \begin{pmatrix} f_x \\ f_y \\ f_z \end{pmatrix}. \quad (2.25)$$

Assume the center of mass for the ith block is (x_0, y_0, z_0). Then we can rewrite Eq. (2.25) as:

$$\Pi_s = -\{D_i\} \begin{pmatrix} f_x S & f_y S & f_z S & [\mathbf{0}]_{\mathbf{9\times 1}} \end{pmatrix}. \quad (2.26)$$

After minimizing the energy equation Eq. (2.26), the subvector of volume loading is formulated as:

$$\begin{pmatrix} f_x S & f_y S & f_z S & [\mathbf{0}]_{\mathbf{9\times 1}} \end{pmatrix}^T \rightarrow \{F_i\}. \quad (2.27)$$

Submatrix of Inertia Force

Denote $(u(t), v(t), w(t))$ as the displacement for any point (x, y, z) in time t. The inertia force per unit volume is:

$$\begin{pmatrix} f_x \\ f_y \\ f_z \end{pmatrix} = -M \begin{pmatrix} \frac{\partial^2 u(t)}{\partial t^2} \\ \frac{\partial^2 v(t)}{\partial t^2} \\ \frac{\partial^2 w(t)}{\partial t^2} \end{pmatrix}, \quad (2.28)$$

where M is the weight density of rock. The potential energy from the inertia force of the ith block is:

$$\Pi_i = -\int\int\int (u\ v\ w) \begin{pmatrix} f_x \\ f_y \\ f_z \end{pmatrix} dx\ dy\ dz = \int\int\int M\{D_i\}^T [T_i]^T [T_i] \frac{\partial^2 \{D(t)\}}{\partial t^2} dx\ dy\ dz. \tag{2.29}$$

We use $\{D(t)\}_{n-1}$ to denote the displacement at previous time-step, $\{D(t)\}_n$ to denote the displacement at current, h to denote the time interval. As the velocity at the end of previous time-step equals velocity at the beginning of current time-step,we have the forward Euler formation:

$$\{D(t)\}_n = \frac{h^2}{2} \frac{\partial^2 \{D(t)\}_{n-1}}{\partial t^2} + h \frac{\partial \{D(t)\}_{n-1}}{\partial t}. \tag{2.30}$$

In the forward Euler method, we consider the acceleration remaining the same within a time-step. Then we have the acceleration vector in current time-step as:

$$\frac{\partial^2 \{D(t)\}_n}{\partial t^2} = \frac{2}{h^2}\{D(t)\}_n - \frac{2}{h}\frac{\partial \{D(t)\}_{n-1}}{\partial t} = \frac{2}{h^2}\{D(t)\}_n - \frac{2}{h}\{V\}_{n-1}, \tag{2.31}$$

where

$$\{V\}_{n-1} = \frac{\partial \{D(t)\}_{n-1}}{\partial t} \tag{2.32}$$

is the velocity at the beginning of a time step. Therefore, Eq. (2.29) can be rewritten as:

$$\Pi_i = \{D_i\}^T \int\int\int [T_i]^T [T_i] dx\ dy\ dz (\frac{2M}{h^2}\{D(t)\}_n - \frac{2M}{h}\{V\}_{n-1}). \tag{2.33}$$

Note that both $\{D_i\}$ and $\{D(t)\}_n$ denote the displacement of current time-step. After minimizing the energy equation with respect to $\{D_i\}^T$, we have:

$$\begin{aligned} \frac{2M}{h^2}\int\int\int [T_i]^T [T_i] dx\ dy\ dz \rightarrow [K_{ii}], \\ \frac{2M}{h}(\int\int\int [T_i]^T [T_i] dx\ dy\ dz)\{V\}_{n-1} \rightarrow \{F_i\}. \end{aligned} \tag{2.34}$$

2.3 Previous Work on DDA Validation

Although the DDA aims to solve very complicated problems, the validation models are actually quite simple. The most widely used validation model is the sliding model, the energy dissipation model, the multi-block model and the tension model, etc. The primary goal of validation is to compare the simulation results with analytical solutions or experimental results, where the difference shows the accuracy of the DDA method.[2,3,10,21–26]

2.3.1 Sliding

The DDA is widely used to simulate blocky systems. One of the most important practical problems DDA aims to solve is the failure of rock systems, which is triggered by sliding of rocks along with

their contact surfaces. As a simplification to this problem, a validation for a sliding block on a frictional incline has been well explored by two-dimensional DDA simulations. The ease to obtain dynamic motions of an object is one of the features that distinguish the DDA from continuum-based methods, which are limited to problems within slow material deformation and few material discontinuities.

The sliding simulation model is shown in Figure 2.2 – a block under gravity slides along a fixed inclined plane with an angle α and an interface friction angle ϕ. In this situation, the analytic solution for the block's displacement as a function of time is

$$d = 1/2at^2 = 1/2(gSin(\alpha) - gCos(\alpha)Tan(\phi))t^2. \tag{2.35}$$

So far, most validated simulation is based on the 2D-DDA model. Yeung[27] studied 12 cases of a sliding model with different combinations of slope angles and friction angles. Yueng also derived an analytical solution for shear and normal contact forces. The difference between analytical results and simulation results was less than 0.5%. Maclauglin and Sitar[28] proposed a 'gravity turn on routine to reduce effects of a sudden loading in the initial time step. There are some other validation models: a block decelerates along an incline with an initial velocity, with a maximum error of 2%;[29] a block with an initial speed stops due to the friction on a horizontal plane, with error less than 0.1%;[30] a block accelerates along a steep slope first and then transfers to a shallower slope decelerating to a stop, and the DDA predicted maximum distance is 5% different from analytical solutions[29,31,32] ; a block slides along an incline with friction and cohesion, where error on

accelerations and contact forces were within 0.02%.[33] Besides, Doolin and Sitar[4] analyzed a 1m $\times 2$m block slides along a 250m plane with an inclined angle $30°$, and addressed the accuracy of the DDA method through a sensitivity analysis.

Simulation results has also been compared with field results. Tsesarsky and Hatzor applied a harmonic oscillation on the original sliding model and a corresponding physical experiment was performed on a larger hydraulic driven shaking table. Then, the DDA simulation results for displacement were compared with experimental results, which showed a similar trend, and the relative error was less than 10%.

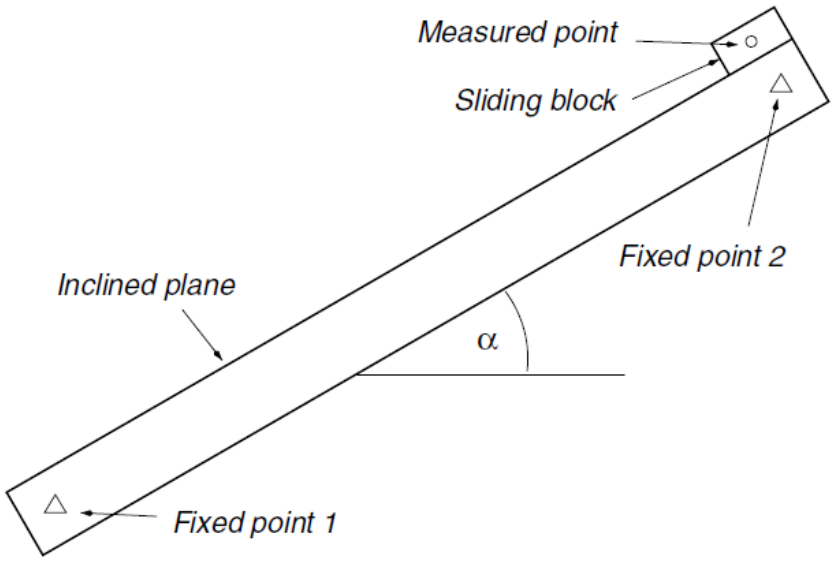

Figure 2.2: The sliding model

M. MacLaughlin and D. Doolin, *Review of validation of the discontinuous deformation analysis (dda) method*, International journal for numerical and analytical methods in geomechanics, vol. 30, no. 4, pp. 271305, 2006. Used under fair use, 2014.

With great effort from many researchers, the 2D-DDA has been well developed and verified. However, two dimensional models are restricted by assuming plane-strain or plane-stress conditions. After Shi proposed a three-dimensional DDA (3D-DDA), a limited number of research work has been done in this new area; this might be because of the very complex contact conditions for arbitrary shaped blocks. Haztor and Bakun-Mazor[3] reviewed current 3D-DDA results, and provided a validation for a sliding block under a Sine horizontal acceleration using the 3D-DDA method. The relative error in terms to block's final position was approximately 8%. The 3D sliding model is shown in Figure. 2.3.

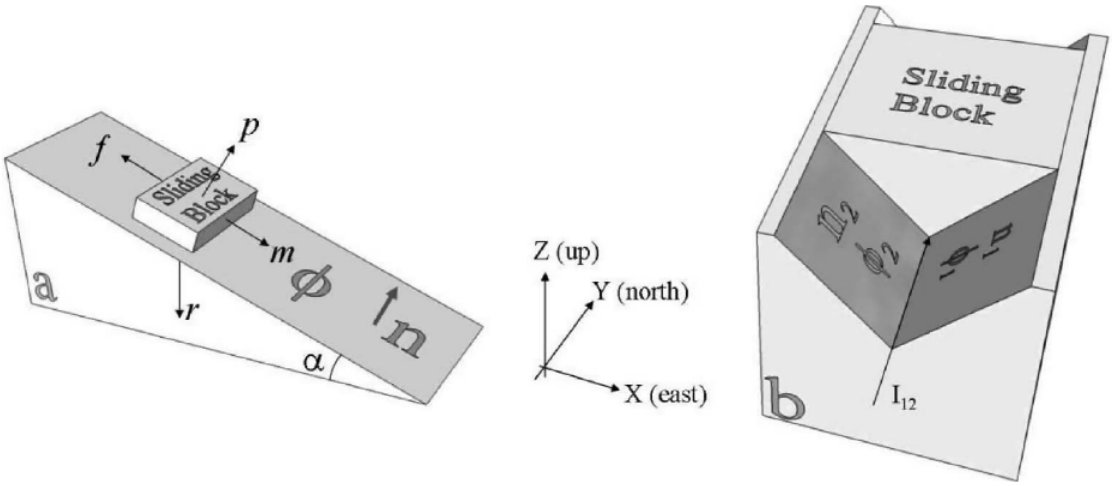

Figure 2.3: **Left:** Single sliding face in 3D. **Right:** Double sliding face in 3D.

Y. Hatzor and D. Bakun-Mazor, *Modelling dynamic deformation in natural rock slopes and underground openings with dda: review of recent results*, Geomechanics and Geoengineering, vol. 6, no. 4, pp. 283292, 2011. Used under fair use, 2014

2.3.2 Energy Dissipation Model

An impacting model is a typical model to test energy dissipation, and it was studied by Shyu[15] through two 2D-DDA simulations: collision between two identical rods and collision between two spheres moving towards each other in opposite directions. The displacement of each object, the velocities of each object and the stress at contact points were recorded and compared with analytical results from Hughes.[34] Then Doolin and Sitar[4] examined a frictionless impact model as Figure 2.4 shows. In their study, a 1m $\times$2 m block falls down freely and hits into a 1m $\times$15 m fixed rod. A heavily damped impact was shown from simulation results. This research also concluded that the rebound is completely damped at very high penalties, and the impact contact forces increase with the sizes of time-step and penalty values.

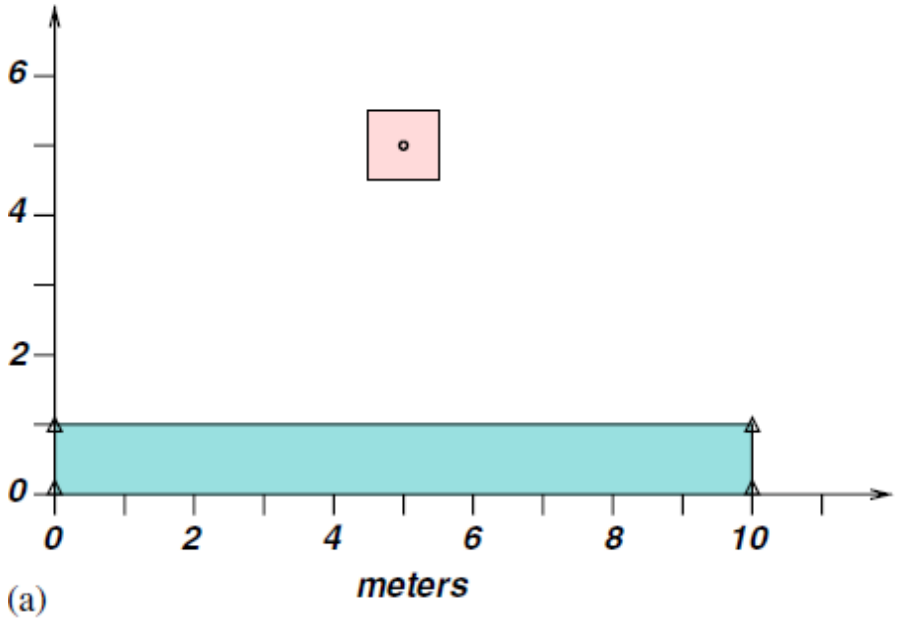

Figure 2.4: Initial position for filling rock tests.

D. M. Doolin and N. Sitar, *Displacement accuracy of discontinuous deformation analysis method applied to sliding block*, Journal of engineering mechanics, vol. 128, no. 11, pp. 11581168, 2002. Used under fair use, 2014.

Energy dissipation has also been studied in time integration scheme analysis. Doolin and Sitar[21] did a comprehensive analysis on time integration for the 2D-DDA, which included a stability analysis and an accuracy analysis for the DDA model. The time scheme applied in DDA ("right Riemann") has advantages of being unconditionally stable and ensure system energy dissipation, but it is implicit and requires expensive iterations to solve. Jiang et al[20] provided an exploration of energy dissipation and convergence criterion for the DDA. Time-step sizes from 0.001s to 0.008s were used to analyze energy dissipation. For convergence criteria, displacement, kinetic energy and unbalanced force from the DDA solution were used for measurements. However, in this research, they only explored the situation that acceleration remains constant during one time-step.

2.4 Challenges

Previous research has exhibited an obvious defect in the DDA: energy dissipation. According to the energy conservation principle, there should be no energy loss in the completely elastic collision. However, loss in energy openly appears in DDA simulations, especially when movement direction changes suddenly. This energy dissipation occurs in the form of velocity and amplitude attenuation even under undamped conditions. In order to overcome this shortcoming, we apply a new time integration scheme to the DDA method: the Newmark method. The improved DDA method will

be testified through a sliding model and an impacting model. Besides, from previous work, we can see that most of DDA work still remains in the 2D level. However, 3D models are important for accuracy of simulations, because the unbalanced bounce and rotation resulting from energy damping in 3D simulation are more obvious than that in 2D. Therefore, 3D-DDA simulations are used in this thesis to simulate block sliding and bouncing.

Chapter 3

Newmark Method in 3D-DDA

In this chapter, we will first introduce the classic Newmark method,[35] and then the applications of the classic Newmark method to the DDA . Also, a new integrated Newmark method are illustrated.

3.1 Newmark Method

The Newmark method is a time-integration method, which shows the relationships between displacement, velocity and acceleration. In each time-step of DDA simulation, the time integration method updates the displacement, velocity and acceleration for every block based on the information of previous time step. Since velocity and acceleration play key roles in forming stiffness matrix in the linear equilibrium equation as mentioned in section 2.2.3, the time-integration method can influence the accuracy of DDA simulation greatly.

Before the illustration of Newmark method in DDA, we will first clarify two set of symbols denoting movement information.

- $\{u\}_n$ describes the accumulated displacement in general case, which denotes the accumulated displacement at the end of current time-step. $\{\dot{u}\}_n$ represents the velocity and $\{\ddot{u}\}_n$ represents the acceleration.

- $\{D(t)\}_n = \{D_i\}$ is the solution of the DDA linear equilibrium equation, and it describes the displacement within current time-step. But $\frac{\partial\{D(t)\}_n}{\partial t}$, $\frac{\partial^2\{D(t)\}_n}{\partial t^2}$ are still the velocity and acceleration respectively: $\frac{\partial\{D(t)\}_n}{\partial t} = \{\dot{u}\}_n$, $\frac{\partial^2\{D(t)\}_n}{\partial t^2} = \{\ddot{u}\}_n$.

Assuming the time interval h is small enough, the velocity vector at the end of current time step $\{\dot{u}\}_n$ is estimated as velocity at the end of previous time step plus acceleration times time interval, and displacement vector at the end of current time-step $\{u\}_n$ is approximated as the sum of displacement at the end of previous time-step, a velocity part and an acceleration part:

$$\{\dot{u}\}_n = \{\dot{u}\}_{n-1} + h\{\ddot{u}\}_\gamma, \tag{3.1}$$

$$\{u\}_n = \{u\}_{n-1} + h\{\dot{u}\}_{n-1} + 1/2h^2\{\ddot{u}\}_\beta, \tag{3.2}$$

where $\{\ddot{u}\}$ is the acceleration vector, and $\{\ddot{u}\}_\gamma$ $\{\ddot{u}\}_\beta$ are accelerations within a time-step:

$$\{\ddot{u}\}_\gamma = (1-\gamma)\{\ddot{u}\}_{n-1} + \gamma\{\ddot{u}\}_n \quad 0 < \gamma < 1, \tag{3.3}$$

$$\{\ddot{u}\}_\beta = (1-2\beta)\{\ddot{u}\}_{n-1} + 2\beta\{\ddot{u}\}_n \quad 0 < 2\beta < 1. \tag{3.4}$$

Hence, the approximation of displacement and velocity are:

$$\{\dot{u}\}_n = \{\dot{u}\}_{n-1} + (1-\gamma)h\{\ddot{u}\}_{n-1} + \gamma h\{\ddot{u}\}_n, \tag{3.5}$$

$$\{u\}_n = \{u\}_{n-1} + h\{\dot{u}\}_{n-1} + (1/2-\beta)h^2\{\ddot{u}\}_{n-1} + \beta h^2\{\ddot{u}\}_n. \tag{3.6}$$

With different values of β and γ, the stability of Newmark method varies:[36] it is conditional stable if $\gamma >= 1/2$, and it is unconditional stable when $\beta >= \frac{1}{4}(\gamma + 1/2)^2$. If taking $\gamma = 1/2$ and $\beta = 1/6$, then the acceleration value $\ddot{u}(t)$ linearly interpolates in the time interval $[t_{n-1}, t_n]$:

$$\{\ddot{u}(t)\} = \{\ddot{u}\}_{n-1} + (t - t_{n-1})\frac{\{\ddot{u}\}_n - \{\ddot{u}\}_{n-1}}{h}. \tag{3.7}$$

Taking $\gamma = 1/2$ and $\beta = 1/4$, then the value of $\{\ddot{u}(t)\}$ is the average acceleration over the time interval $[t_{n-1}, t_n]$:

$$\{\ddot{u}(t)\} = \frac{\{\ddot{u}\}_{n-1} + \{\ddot{u}\}_n}{2}. \tag{3.8}$$

3.2 Newmark Method in DDA

As a time-integration scheme, the Newmark method is used to approximate blocks' movement information (displacement, velocity and acceleration) of current time-step based on that of previous time-step. For DDA simulation, there are two parts need movement information: one is developing

submatrix of inertia force, another one is updating movement's information at the end of each time-step.

To develop the submatrix of inertia force for a block, $(u(t), v(t), w(t))$ are used to denote the displacements at any point (x, y, z) in the time t. Then the inertia force per unit volume is given by a product of weight density and acceleration:

$$\begin{pmatrix} f_x \\ f_y \\ f_z \end{pmatrix} = -M \begin{pmatrix} \frac{\partial^2 u(t)}{\partial t^2} \\ \frac{\partial^2 v(t)}{\partial t^2} \\ \frac{\partial^2 w(t)}{\partial t^2} \end{pmatrix}, \tag{3.9}$$

Then the potential energy from the inertia force of the ith block can be denoted as an integration of product of displacement and inertia force over volume:

$$\Pi_i = -\int\int\int (u\ v\ w) \begin{pmatrix} f_x \\ f_y \\ f_z \end{pmatrix} dx\ dy\ dz = \int\int\int M\{D_i\}^T [T_i]^T [T_i] \frac{\partial^2 \{D(t)\}}{\partial t^2} dx\ dy\ dz. \tag{3.10}$$

Take $\{D(t)\}_{n-1}$ to denote the DDA displacement in the previous time step, $\{D(t)\}_n$ to denote the displacement increment in the current time step, h to denote the time interval. Then applying the Newmark method:

$$\frac{\partial^2 \{D(t)\}_n}{\partial t^2} = \frac{1}{h^2\beta}\{D(t)\}_n - \frac{1}{h\beta}\frac{\partial \{D(t)\}_{n-1}}{\partial t} - \frac{(1/2-\beta)}{\beta}\frac{\partial^2 \{D(t)\}_{n-1}}{\partial t^2}, \tag{3.11}$$

$$\frac{\partial\{D(t)\}_n}{\partial t} = \frac{\partial\{D(t)\}_{n-1}}{\partial t} + (1-\gamma)h\frac{\partial^2\{D(t)\}_{n-1}}{\partial t^2} + \gamma h\frac{\partial^2\{D(t)\}_n}{\partial t^2}. \tag{3.12}$$

Replace the acceleration in the energy equation with Newmark acceleration, Eq. (3.10) can be rewritten as:

$$\Pi_i = \{D_i\}^T \int\int\int [T_i]^T[T_i]dx\,dy\,dz(\frac{[M]}{h^2\beta}\{D(t)\}_n - \frac{[M]}{h\beta}\frac{\partial\{D(t)\}_{n-1}}{\partial t} - \frac{(1/2-\beta)[M]}{\beta}\frac{\partial^2\{D(t)\}_{n-1}}{\partial t^2}). \tag{3.13}$$

As $\{D(t)\}_n = \{D_i\}$, minimizing the energy equation Eq. (3.13) with respect to $\{D_i\}^T$, we have the stiffness submatrix and force sub-vector resulting from inertial force as:

$$\begin{aligned}(\int\int\int [T_i]^T[T_i]dx\,dy\,dz)A &\to [K_{ii}],\\ (\int\int\int [T_i]^T[T_i]dx\,dy\,dz)B &\to \{F_i\},\end{aligned} \tag{3.14}$$

where

$$\begin{aligned}A &= \frac{[M]}{h^2\beta},\\ B &= (\frac{[M]}{h\beta}\frac{\partial\{D(t)\}_{n-1}}{\partial t} + \frac{(1/2-\beta)[M]}{\beta}\frac{\partial^2\{D(t)\}_{n-1}}{\partial t^2}).\end{aligned} \tag{3.15}$$

With Eq. (3.14)and Eq. (3.15), the Newmark method has been applied in the DDA method to acquire the submatrix of inertia force.

3.3 The Energy Balance of the Newmark Method in DDA

The following part will prove the energy balance of the Newmark method in DDA method. Simplifying the DDA model as a particle without regarding the stress and strain, then only point loading and inertial force is considerate:

$$\{D_n\} = (h\frac{\partial\{D(t)\}_{n-1}}{\partial t} + h^2(1/2-\beta)\frac{\partial^2\{D(t)\}_{n-1}}{\partial t^2}) + h^2\beta\frac{\partial^2\{D(t)\}_n}{\partial t^2}[M]. \tag{3.16}$$

For the traditional Newmark method, Krenk[37] has proved its balance in energy. He denotes the energy change in one time-step as:

$$(1/2\{\dot{u}\}^T[M]\{\dot{u}\} + 1/2\{u\}^T[K]\{u\})_{n-1}^n. \tag{3.17}$$

After combing Eq. (3.17) with Newmark method Eq. (3.1), (3.2), then a reformulation of energy change in one time-step is obtained as

$$\begin{aligned}&(1/2\{\dot{u}\}^T[M]\{\dot{u}\} + 1/2\{u\}^T([K] + (\beta-1/2\gamma)h[K][M]^{-1}[K])\{u\})_{n-1}^n \\ &= -(\gamma-1/2)\{D\}^T([K] + (\beta-1/2\gamma)h[K][M]^{-1}[K])\{u\})\{D\},\end{aligned} \tag{3.18}$$

where the the original stiffness matrix can be replaced as an equivalent stiffness matrix: $[K]_{eq} = [K] + (\beta - 1/2\gamma)h[K][M]^{-1}[K])$. Note that if we take $\beta = 1/4$ in Eq. (3.16), then the solution of DDA would be the same as the Newmark method taking $\beta = 1/4, \gamma = 1/2$, where Eq. (3.18) suggests no energy dissipation.

3.4 The Integrated Newmark Method in DDA

Besides the classic Newamrk method, an integrated Newmark method is developed and applied to the DDA method. Unlike the classic Newmark method, velocity and acceleration information are not required for the integrated Newmark method when the linear equilibrium equation is developed.

The general kinetic function is:

$$[M]\{\ddot{u}\} + [C]\{\dot{u}\} + [K]\{u\} = \{P\}, \tag{3.19}$$

where $\{u\}$ is the accumulated displacement, [M] is the mass matrix, [C] is the damping matrix, [K] is the stiffness matrix without considering the inertia force and $\{P\}$ is the loading matrix without inertia force. In order to convert the unknown variable $\{u_n\}$ to displacement at each time step $\{D_n\}$, considering the following four equations of four time-step under undamped situation:

$$[M]\{\ddot{u}\}_n + [K]\{u\}_n = \{P\}_n, \tag{3.20}$$

$$[M]\{\ddot{u}\}_{n-1} + [K]\{u\}_{n-1} = \{P\}_{n-1}, \tag{3.21}$$

$$[M]\{\ddot{u}\}_{n-2} + [K]\{u\}_{n-2} = \{P\}_{n-2}, \tag{3.22}$$

$$[M]\{\ddot{u}\}_{n-3} + [K]\{u\}_{n-3} = \{P\}_{n-3}. \tag{3.23}$$

After reorganizing equations as (Eq. (3.21)+Eq. (3.20))-(Eq. (3.22)+Eq. (3.23)), we have :

$$[M][(\{\ddot{u}\}_n + \{\ddot{u}\}_{n-1}) - (\{\ddot{u}\}_{n-2} + \{\ddot{u}\}_{n-3})] + [K][\{u\}_n + \{u\}_{n-1} - \{u\}_{n-2} - \{u\}_{n-3}]$$
$$= \{P\}_n + \{P\}_{n-1} - \{P\}_{n-2} - \{P\}_{n-3}. \tag{3.24}$$

As taking the newmark method is unconditional stable when $\gamma = 1/2$ and $\beta = 1/4$,[36] we formulate the Newmark method as:

$$\{\dot{u}\}_n = \{\dot{u}\}_{n-1} + 1/2h(\{\ddot{u}\}_{n-1} + \{\ddot{u}\}_n), \tag{3.25}$$

$$\{u\}_n = \{u\}_{n-1} + h\{\dot{u}\}_{n-1} + 1/4h^2(\{\ddot{u}\}_{n-1} + \{\ddot{u}\}_n). \tag{3.26}$$

Then, after Eq. (3.25) and Eq. (3.26) are combined, we have:

$$\{\ddot{u}\}_n + \{\ddot{u}\}_{n-1} = \frac{4}{h^2}(\{u\}_n - \{u\}_{n-1}) + \frac{4}{h}\{\dot{u}\}_{n-1}. \tag{3.27}$$

We can also obtain a reorganization, $2\times$Eq. (3.26) - Eq. (3.25), as:

$$\frac{\{u\}_n - \{u\}_{n-1}}{h} = \frac{\{\dot{u}\}_n + \{\dot{u}\}_{n-1}}{2}. \tag{3.28}$$

With Eq. (3.27) and Eq. (3.28), we can reformulate Eq. (3.24). The part of mass matrix $[M]$ in

Eq. (3.24) can be rewritten as:

$$\begin{aligned}
&[M][(\{\ddot{u}\}_n + \{\ddot{u}\}_{n-1}) - (\{\ddot{u}\}_{n-2} + \{\ddot{u}\}_{n-3})] \\
&= [M]\{\frac{4}{h^2}(\{D\}_n - \{D\}_{n-2}) - \frac{4}{h}(\{\dot{u}\}_{n-1} - \{\dot{u}\}_{n-3})\} \\
&= [M]\{\frac{4}{h^2}(\{D\}_n - \{D\}_{n-2}) - \frac{4}{h}[(\{\dot{u}\}_{n-1} + \{\dot{u}\}_{n-1}) - (\{\dot{u}\}_{n-1} + \{\dot{u}\}_{n-3})]\} \\
&= [M]\{\frac{4}{h^2}(\{D\}_n - 2\{D\}_{n-1} + \{D\}_{n-2})\},
\end{aligned} \tag{3.29}$$

where:

$$\begin{aligned}
\{D\}_n &= \{u\}_n - \{u\}_{n-1}, \\
\{D\}_{n-1} &= \{u\}_{n-1} - \{u\}_{n-2}, \\
\{D\}_{n-2} &= \{u\}_{n-2} - \{u\}_{n-3}.
\end{aligned} \tag{3.30}$$

The part of stiffness matrix $[K]$ in Eq. (3.24) can also be rewritten as:

$$\begin{aligned}
&[K][\{u\}_n + \{u\}_{n-1} - \{u\}_{n-2} - \{u\}_{n-3}] \\
=&[K][(\{u\}_n - \{u\}_{n-2}) + (\{u\}_{n-1} - \{u\}_{n-3})] \\
=&[K][(\{D\}_n + \{D\}_{n-1}) + (\{D\}_{n-1} + \{D\}_{n-2})].
\end{aligned} \tag{3.31}$$

Finally, substituting Eq. (3.29) and Eq. (3.31) into Eq. (3.24), the equation of displacement in

each time-step can be formulated as:

$$\begin{aligned}&[M]\{\frac{4}{h^2}(\{D\}_n - 2\{D\}_{n-1} + \{D\}_{n-2})\} + [K][(\{D\}_n + \{D\}_{n-1}) + (\{D\}_{n-1} + \{D\}_{n-2})]\\&= \{P\}_n + \{P\}_{n-1} - \{P\}_{n-2} - \{P\}_{n-3}.\end{aligned} \tag{3.32}$$

As $\{D\}_n$ is the unknown variable, we reformulate Eq. (3.32) as:

$$\begin{aligned}&[M]\frac{4}{h^2}\{D\}_n + [K]\{D\}_n\\=&[M](\frac{4}{h^2}(2\{D\}_{n-1} - \{D\}_{n-2}) - [K](2 \times \{D\}_{n-1} + \{D\}_{n-2})\\&+ \{P\}_n + \{P\}_{n-1} - \{P\}_{n-2} - \{P\}_{n-3}.\end{aligned} \tag{3.33}$$

Therefore, the submatrix of inertia force – stiffness submatrix and force subvector resulting from inertia force – are:

$$\begin{aligned}&[M]\frac{4}{h^2} \rightarrow [K_{ii}],\\&[M](\frac{4}{h^2}(2\{D\}_{n-1} - \{D\}_{n-2}) \rightarrow [F_i].\end{aligned} \tag{3.34}$$

Also, the following part are required to be added to force vector in the global equation:

$$-[K](2 \times \{D\}_{n-1} + \{D\}_{n-2}) + \{P\}_{n-1} - \{P\}_{n-2} - \{P\}_{n-3} \rightarrow [F_i]. \tag{3.35}$$

At this point, the Eq. (3.34) and Eq. (3.35) contend all the inertial force information that linear equilibrium equation requires.

Chapter 4

Implement Details

So far, there is no sophisticated open source 3D-DDA code for simulating irregular shaped blocks. Thanks to Professor Peng from China water and hydra resource institute, who contributed his private 3D-DDA code, our experiment can be conducted based on it. The 3D-DDA code is an extensible code developed in FORTRAN, and it is focused on implement of 3D-DDA Algorithm. Because of the difficulty in 3D DDA simulation, this code is one of the few codes that able to simulate the entire process of 3D block movements. But there are several challenges in revising this code. The main problem is that the structure of this code is not well organized – its first version was developed twenty years ago, and the optimization for this code are based on the first version's structure. Therefore, this code is not object-oriented, the entire code is just in one file.

4.1 Structure of the DDA Code

Because of the confusion of the code's structure, it is necessary to understand the mechanism of entire code. The Figure. 4.1 shows the a big picture of the DDA algorithm, including inputting the block structure information, generating the stiffness matrix, solving the equation and checking the contacts information. We will illustrate the structure of the DDA code through the following functions:

- `READ_PXC()` is a function to read input files. There are two input files: `Good.txt` and `info.txt`. The block structure information is stored in `Good.txt` , which includes the surface number in each block, the point label in each surface, point coordinates, and equation parameters for each surface. Other parameters are stored in the file `Good.txt` , including Poisson ratio, Young's modulus, gravity, etc.

- `STIFF()` is a function to determine the global stiffness matrix and right-side loading vector in the linear equilibrium equation resulting from point load, volume load, initial stress, block interactions. The theoretical details has been presented in section 2.2. The results are stored in a $6n \times (6n + 1)$ matrix called `ff()`, where n is the number of unfixed blocks. In `ff()`, the first $6n \times 6n$ matrix stores the stiffness matrix information, and the last column is the right-side loading vector.

- `GXSTIFF()` obtains the information of the submatrix of inertia force, and then adds it to the global matrix `ff()`.

- `SOLVER_PCG_zgx()` applies preconditioned conjugate gradient (PCG) method to solve the linear equilibrium equation, and the solution are the displacement and rotation of unfixed blocks, which store in a $6n$ vector called `ee()`. However, in case of bad convergence rate for PCG, a `SOLUT3 ()` function employing the classic Gaussian elimination method will be applied to resolve the linear equilibrium equation.

- `NEWLOCATION()` `MACLENG()` `MAXMIN()` `MAXMINPLANE()` check the contacts information when new location of unfixed blocks has been solved from the linear equilibrium equation. If the new location of blocks are not satisfied with the contacting law, such as tensile force existing between blocks, then the stiffness matrix need to be redeveloped. A variable called `MCBH` records the friction status; if the friction status changes, the stiffness matrix will also be recalculated. The stiffness matrix maybe regenerated several times, and the simulation would not step into the next time-step unless the solution of equilibrium equation satisfies all contacting laws.

- `DT()` is a function to export the blocks' coordinate information and to update other information, such as velocity and acceleration. It will only be called once at the end of every time-step.

There are also quit a large number of functions to handle the details, such as `T_DELT()` to adjust time-step size, `MIDJL` to record error information.

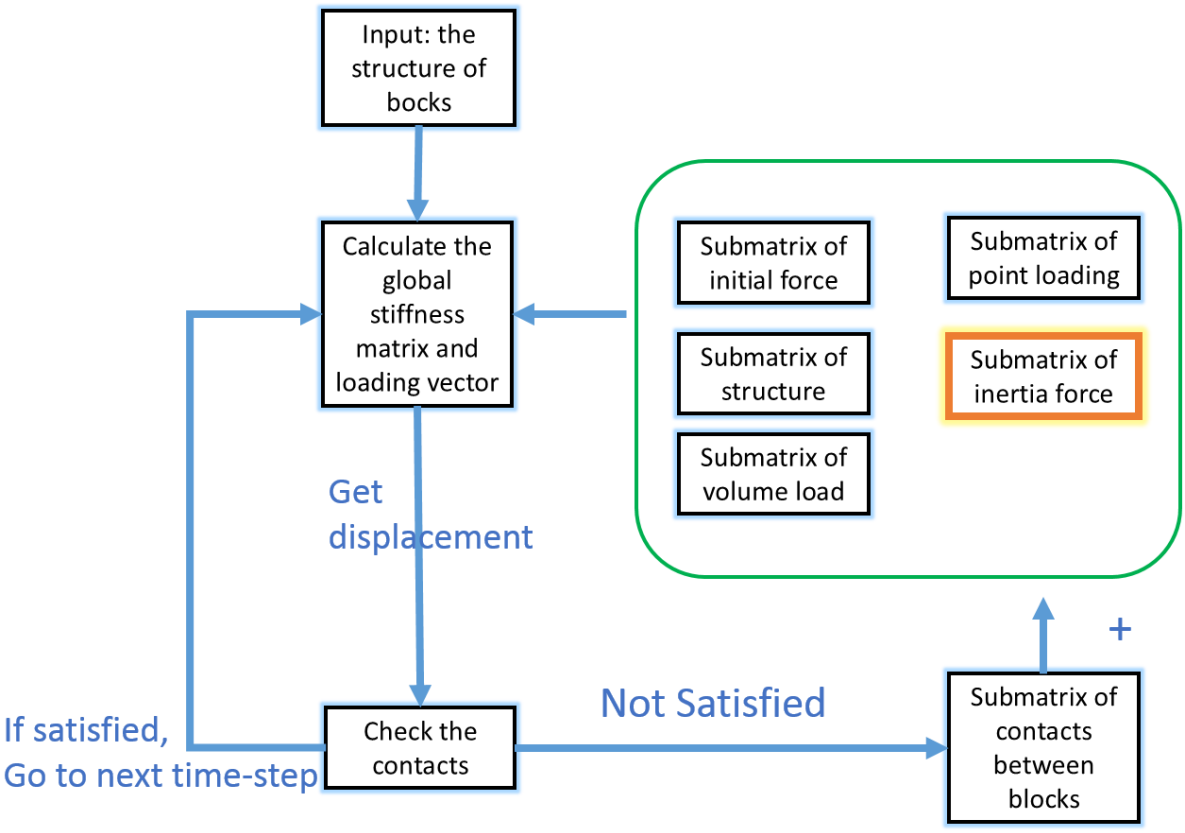

Figure 4.1: Flowchart for the DDA code

4.2 Newmark Method in the DDA Code

Note that the submatrix of inertial force is the only part related with time integration method; therefore, to apply newmark method into DDA code, function `GXSTIFF()` is the key part to revise. After we Applied Eq. (3.14) and Eq. (3.15) to the DDA code, the following part is the Newmark method in `GXSTIFF()` function:

```
SUBROUTINE GXSTIFF(IMBF)


DMF=4./DELT

DMK=DMF/DELT


DO 1900 KBLOCK=1,NBLOCK


IF (KBLOCK.EQ.1) IDENT=0

IJ=ISTRI(2,KBLOCK)

IF (IJ.EQ.0) GOTO 1900


CALL TV(DIU,KBLOCK)

FI=0.0

DO I=1,6
```

```
DO J=1,6

FI(I)=FI(I)+FFS(I,J,KBLOCK)*DIU(J)*GAMA

ENDDO

ENDDO



DO I=1,6

DO J=1,6

KII(I,J)=FFS(I,J,KBLOCK)*DMK*GAMA

ENDDO

ENDDO



CALL DRZKII(KBLOC,KII,FI)



1900 CONTINUE

RETURN

END
```

The function `GXSTIFF()` is the last part to form the global stiffness matrix, and it runs after `STIFF()`. The return value of `TV()` is a vector `DIU(6)`, storing the value of $(4\frac{\partial[D(t)_{n-1}]}{\partial t} - 2\frac{\partial^2[D(t)_{n-1}]}{\partial t^2})$ of the `KBLOCK`'s object. `FFS()` is the mass matrix, which is $[M]$ in Eq. (3.14) and Eq. (3.15). After the submatrix of inertial force has been acquired, a function `DRZKII ()` will

map the local stiffness matrix into the global matrix.

Besides the `GXSTIFF()`, the velocity and acceleration should be updated at the end of each time-step:

```
ACCEL()=4./DELT/DELT*DIU()-4./DELT*VEL_1()-ACCEL_1()
VEL()=VEL_1()+0.5*DELT*(ACCEL_1()+ACCEL())
```

4.3 Implement of the Integrated Newmark Method in the DDA Code

Apply the integrated Newmark method into DDA code is more complicated. Because the loading vector of current time-step relies on the loading vectors in previous time-step, and the equation is deducted based on the assumption that the mass matrix $[M]$ and stiffness matrix $[K]$ remain the same in recent four time-steps. As a result, the Newmark method can not be applied during the whole process. As $[M]$ is only related with the structure of block, $[M]$ does not change during the entire simulation process. However, $[K]$ changes whenever the contacts vary. Therefore, once contact status changes, the forward Euler method will be applied. After contacts status keep the same for three time-steps, Newmark method will be applied again. This process is shown in Figure 4.2.

The function `GXSTIFF()`, which is used for obtaining the submatrix of inertial force, is the key part to apply the integrated Newmark method. This part is based on the Eq. (3.34) and Eq. (3.35).

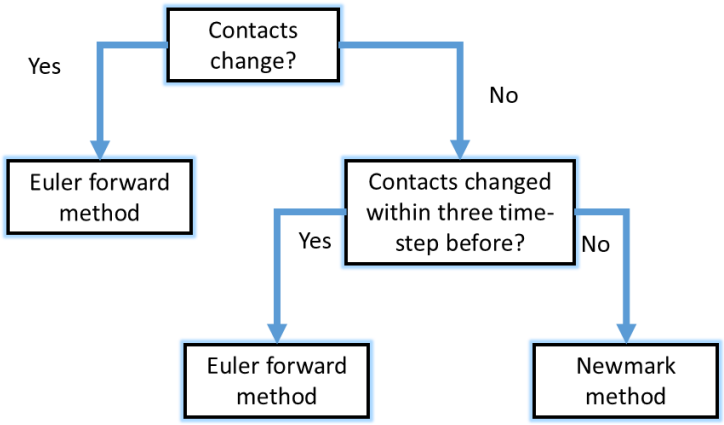

Figure 4.2: Switch between the forward Euler method and the Newmark method

But through Eq. (3.20) to Eq. (3.23), it clearly shows that both the loading vector $\{P\}$ and the stiffness matrix $[K]$ are the global information without considering the inertial force. Therefore, close attentions are paid when updating the stiffness matrix and the loading vector. Figure. 4.3 shows the flowchart of how `GXSTIFF()` works.

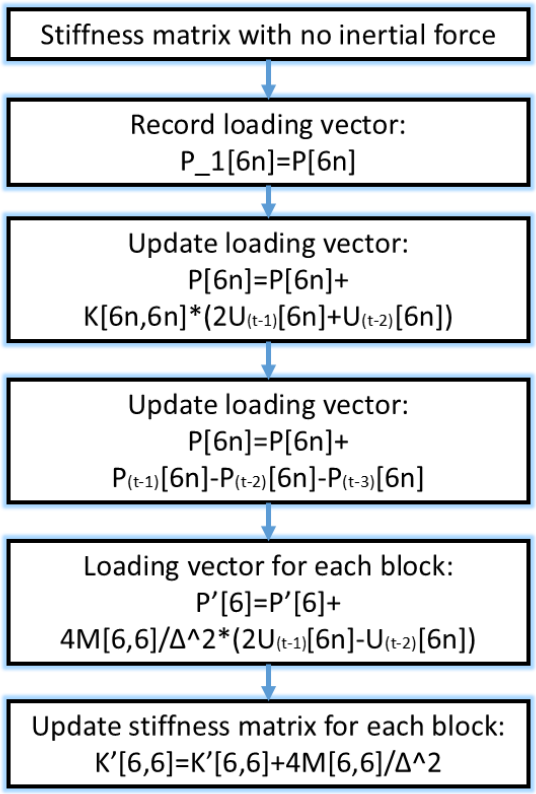

Figure 4.3: Flowchart for GXSTIFF() function in DDA code

Chapter 5

Results and Analysis

In this chapter, we will report the simulation results for two DDA models. The first model is a sliding model, which composed of a fixed incline and a small block. The second model is an impacting model, in which a small block impacts a fixed horizontal surface. As the DDA is designed for solving discrete systems, contacting between objects can be regarded as the most important part in simulation. A contact is composed of a tangential direction contact and a normal direction contact. A sliding model is a great example for simulating tangential contacts and an impacting model is for normal contacts. Therefore, both models are the very fundamental for DDA verification. The general structures of these two models are illustrated, and the experiment results will be shown.

To show the accuracy improvements by the Newmark method, the forward Euler method is used for comparison. Before this study, the forward Euler method is the only time-integration scheme

applied in the DDA simulation. It is a very stable method, while resulting in strong damping effects at the same time.[21] This damping effect becomes more obvious when a sudden change of movement direction occurs.

The DDA code we use is offered by Professor Peng from China Institute of Water Resource and Hydropower Research, and it is developed by Fortran. After models have been developed, the displacement of the center of block is used to compare the accuracy of two different time integration methods. So far, most research in DDA are restricted to two dimensional simulation, but in this study both models are three dimensional models with six degree of freedoms – displacement in x,y,z directions and rotation in x,y,z directions. The three dimensional results will be compared with analytical solution, and the relative error will be measured.

5.1 Sliding Model

A sliding model represents a simplified model to simulate rocks sliding along structure surfaces, as they share similar boundary conditions: the rock(block) slides in the direction of slope with no restriction in other direction.

The points of this experiment are: 1) to validate the 3D-DDA method through comparison between analytically solution and simulation solution, 2) to compare the accuracy of the Newmark method and the forward Euler method, 3) to explore the computational costs for these two time-integration method.

In this study, a $0.3m \times 0.3m \times 0.3m$ three dimensional block lies on a fixed 30 degrees slope, as Figure 5.1 shows. Each experiment lasts 1.5 second in simulation time, which is the summation of all time-step. At the start point, a small block is released from the top of slope with zero initial velocity. After a very short period of stabilizing, the block will slides along the frictionless slope smoothly. The only force applied to the small block is the gravity. During the process, displacement and time are recorded.

The material parameters for the block are: Young's modulus $E = 1MPa$, Poisson's ratio $v = 0.7$, and unit weight $\gamma = 2.7KN/m^3$. The interface properties are: frictional angle $\phi = 0°$, cohesion $C = 0$, and normal contact stiffness $p_n = 3 \times 10^7$.

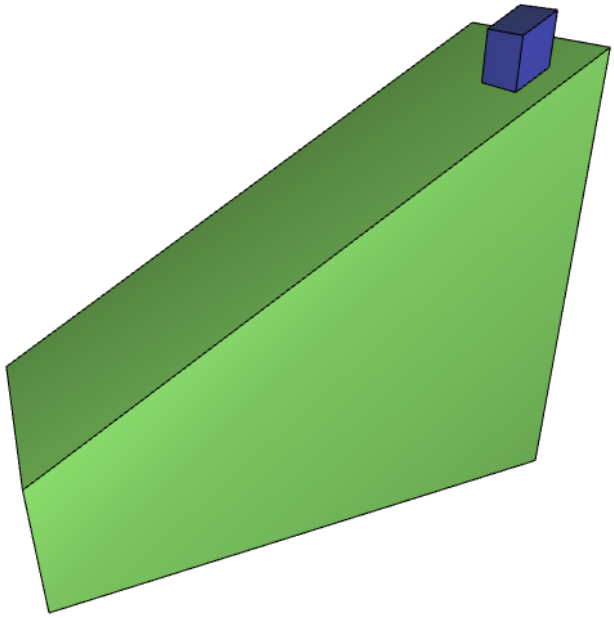

Figure 5.1: Sliding model: a small block sliding along a fixed slope

5.1.1 Accuracy Analysis

To validate the DDA method, a simulation of sliding model was conduct. For this simulation, the time-step is fixed as 0.002s, and the trajectory of small block within a total 1.5s simulation time were recorded. Figure 5.2 displays the results: a comparison between DDA solution using the forward Euler time integration, DDA solution using the Newmark time integration and the analytical solution. The picture shows that the displacement of DDA method using both time integration schemes are very close to the analytical solution:

$$d = \frac{1}{2}g(sin(\alpha) - cos(\alpha)tan(\phi))t^2 \tag{5.1}$$

where d is the displacement, α is the degree of slope, ϕ is the frictional angle which is zero here, t is the accumulated time. To measure the accuracy of the forward Euler method and the Newmark method, we define a relative error as:

$$E_r = (D_s - D_a)/D_a \tag{5.2}$$

where E_r is the relative error, D_s is the simulated displacement and D_a is the analytical displacement. Figure 5.3 illustrates the relative error based on the same results of Figure. 5.2. It shows that the beginning of DDA simulation is not very stable, and relative errors change quickly. That is because the block adjusts itself to a stable condition when it contacts with the slope at the very beginning. But after the block starts to slide steadily along the slope, the relative errors for both

time integration methods decrease smoothly. The relative error at the end of 1.5s is less than 0.3%.

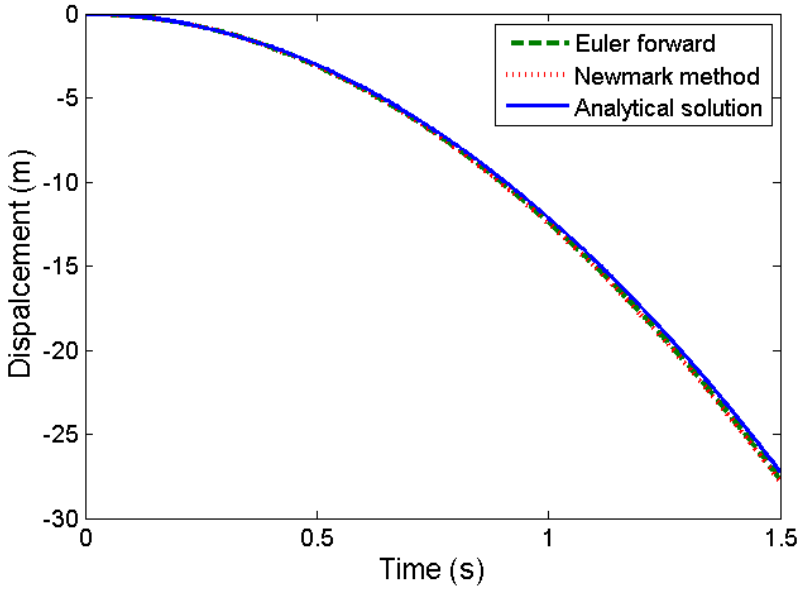

Figure 5.2: Displacement-time relationship for the sliding model. With size of timestep 0.002s, both the forward Euler method and the Newmark method provide solutions very close to the analytical solution.

The size of time-step influences the accuracy of simulation results directly. To examine the accuracy of the DDA method in respect of time-step size, seven individual sliding tests with different sizes of time-steps (0.002s, 0.004s, 0.008s, 0.016s, 0.02s, 0.025s, 0.032s) were applied in the sliding model. For each tests, they had the same initial conditions, boundary conditions, and the entire simulations last 1.5s in real time. The error at final point is used as the relative error value for each test. From the Figure 5.4 we can see that when time-step $h = 0.002, 0.008, 0.016$, the Newmark method presents a higher relative error. While for the rest $h = 0.004, 0.020, 0.025, 0.032$, the Newmark method leads to a better accuracy. This picture also shows that the error of the forward Euler method is linear related with time-step size, but the error of the Newmark method is not.

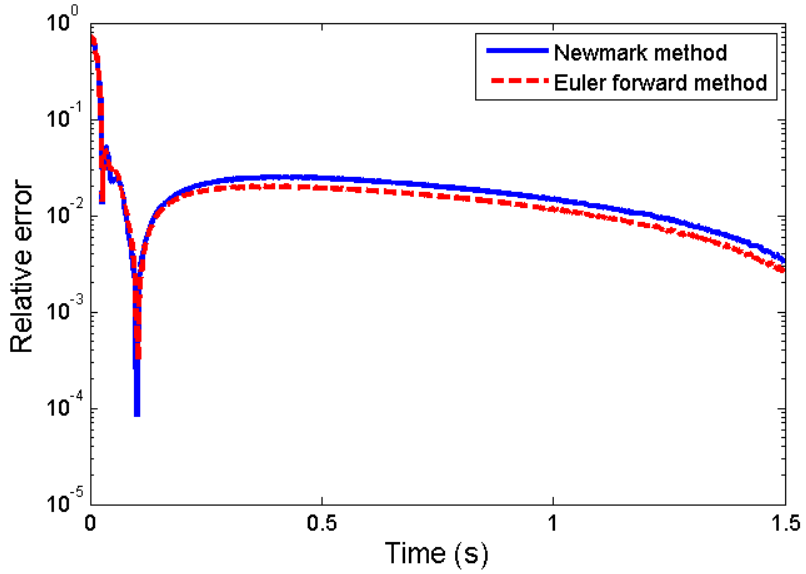

Figure 5.3: Relative error and time relationship for the sliding model. The relative errors of both the Newmark method and the forward Euler method decline steadily after a point.

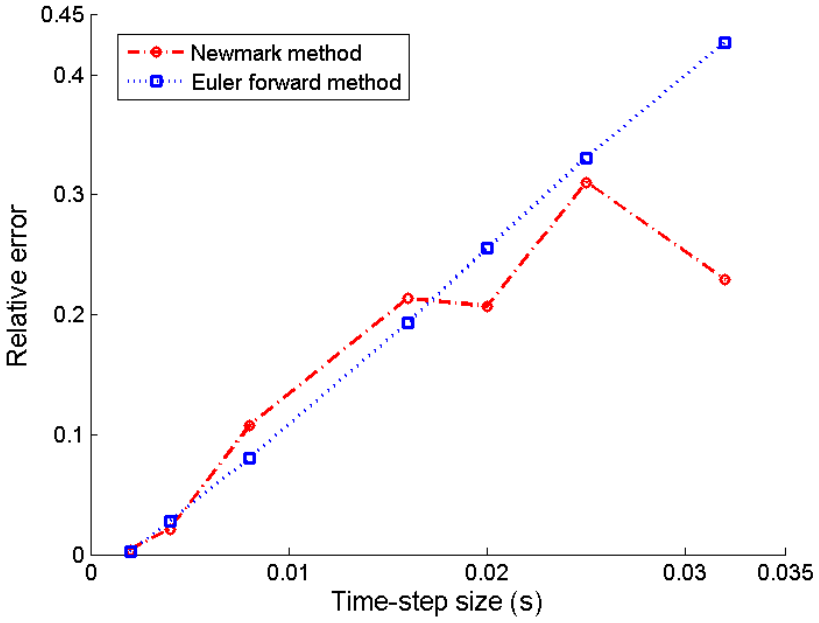

Figure 5.4: Time-step size and relative error relatioship for the sliding model. The comparison is based on simulation solutions which have the same simulatation time (1.5 s)

5.1.2 Computational Time Comparison

Figure 5.5 shows the computational cost of the DDA code using the Newmark method and the forward Euler method. The computational time of six independent tests with different numbers of time-steps (60, 75, 188, 375, 750, 1500) were recorded. All the simulations start at a same initial point, have the same boundary condition and the same simulation time 1.5s. The different numbers of time-steps (n) are achieved by the change of time-step size (h) in the sliding model. From the figure, we can see that the simulations using the Newmark method and the forward Euler method cost almost the same computational time. This is because time integration is only a small part in the entire DDA code. Also, besides the way to obtain velocity and acceleration, the rest algorithm of these two time integration methods are very similar.

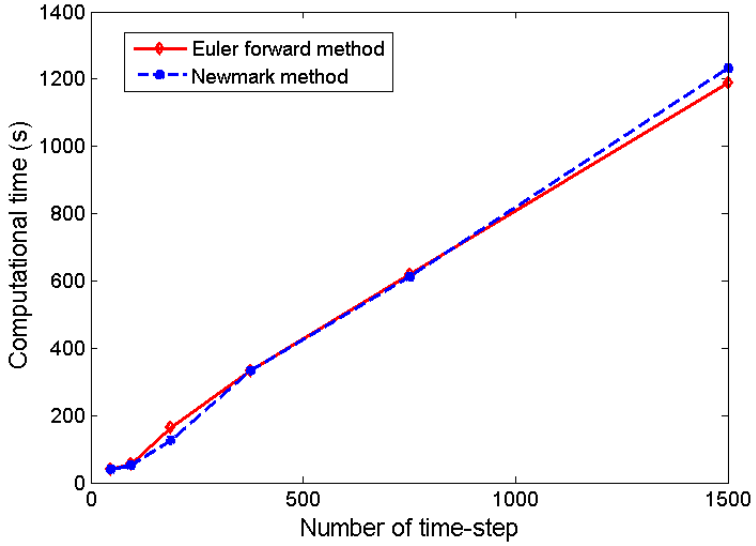

Figure 5.5: Model size (timestep number) and computational costs relationship in sliding model. The computational time for the Newmark method and the forward Euler method are almost the same.

5.2 Impacting Model

Impacting model is composed of a fixed surface and a small block which can move freely. It is a very important validation model for DDA simulation to test how normal contacts between blocks work, and how they work under condition of trajectory direction changes rapidly. The impacting process in simulation can be classified as two part: contacting and non-contacting parts. When blocks contact with each other, they are connected by two artificial springs: a normal one and a tangential one. When blocks are not contacting, they moves independently, and the only force the small block took is the gravity.

As the direction of movements change during a relatively small time of contacting in the impacting model, strong damping effects occur even in undamped cases when the forward Euler method is applied. This is against the theoretical solution, because there is no energy dissipation shown in the DDA equation. Being a challenge in the DDA simulation for a long time, the unreasonable damping effects can be vanished by applying the Newmark method, and it will greatly increase the accuracy of the DDA.

The points of this experiment are: 1) to demonstrate the significant accuracy improvements through using the Newmark method, 2) to explore how the time-step size effects the accuracy of the forward Euler method and the Newmark method.

The impacting model is composed of a $3m \times 3m \times 3m$ small block and a $10m \times 10m \times 10m$ big block, as Figure 5.6 shows. The big block is fixed, and the small one can move freely. In the simulation, the small block falls down at the point of $0.3m$ above the big one, and then constantly

impacts the big block until being stop. A total 1.0 second real time movement of impacting model is simulated. During the process, displacement, velocity and acceleration are recorded. The material parameters og the block are: Young's modulus $E = 1MPa$, Poisson's ratio $v = 0.7$, and unit weight $\gamma = 2.7KN/m^3$. The interface properties are: frictional angle $\phi = 0°$, cohesion $C = 0$, and normal contact stiffness $p_n = 3 \times 10^7$.

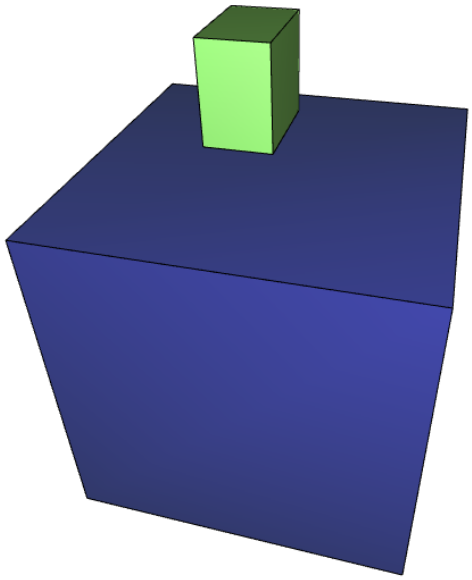

Figure 5.6: Impacting model: a small block falling down and constantly impacting a fixed block

5.2.1 Damping Effects

Damping effect is the influence to shrinkage the amplitude of oscillation. But the continuous oscillation is very difficult to simulate in the discrete system, thus, the impacting model is applied as the substitution.

In this study, three time integration methods are going to be explored: the forward Euler method, the classic Newmark method and the integrated Newmark method. The simulation results of displacement, velocity and acceleration are compared with analytical results:

$$\Delta d = v \times h + \frac{1}{2} \times a \times h^2. \tag{5.3}$$

This is the analytical solution for a one dimensional problem, and the object is idealized as a particle. This situation is usually simulated by a Single-degree of freedom system in previous research.[20,21] However, in the 3D-DDA simulation, we use a six degree of freedom model: the small block will impact the fixed surface with its entire bottom plane, and it is possible to rotate or move to any direction.

In this experiment, the bottom plane of the small block is parallel to the fixed ground surface, and no friction is applied in contacts. As the small block shows barely any offset in Y,Z direction, only the vertical trajectory of its mass center is recorded for comparison analysis. Figures 5.7-5.9 demonstrate the comparison results. Figure 5.7 is the displacement comparison, it shows that the forward Euler method results in a strong damping effect, the solution of classic Newmark method matches well with analytical solution, and the integrated Newmark method amplifies oscillation. Even though the classic Newmark solution is very close to the analytical solution, it still shows a slight damping, as its peak is lower than analytical one in the fourth impacting loop. Figure 5.8 is the velocity comparison. In this figure, it shows that the damping effects in the forward Euler method mainly occurs when two blocks contacting to each other, while the amplifying effects in

the integrated Newmark method imbedded in the entire process – both when two blocks contact and separate. We believe this is an inner defect of the integrated method, but the reason is not clear yet. Figure 5.9 shows the acceleration information: their peak values, which happen in contacting, demonstrate how stable for the impacting process. Peaks in the forward Euler method decrease linearly, those in the classic Newmark method keep the same in each loop, and that in the integrated Newmark method have no stable trend.

Generally speaking, the integrated Newmark method does not show a good match with analytical solution. But so far, we do not know the reason. It might be because of the defects in either equation deduction or the code. Therefore, the rest analysis will not include Integrated Newmark method.

Figure 5.10 shows the energy change in the impacting process, which verifies the energy conservation of the Newmark method. It also shows a damping effect in forward Euler method and an amplifying effect in the integrated Newmark method.

5.2.2 Time-step effects

Time-step is closely related with the accuracy of a simulation. Figures 5.11-5.13 show the impacting model simulation results when different time-step sizes (0.0005s, 0.0015s, 0.0025s, 0.004s) are applied. From these four Figures, we can tell that damping effects from the forward Euler method increasing with increment of time-step size. For the Newmark method, the solution matches with analytical solution reasonable well when time-step size equals to 0.0005s, 0.0015s and 0.0025s,

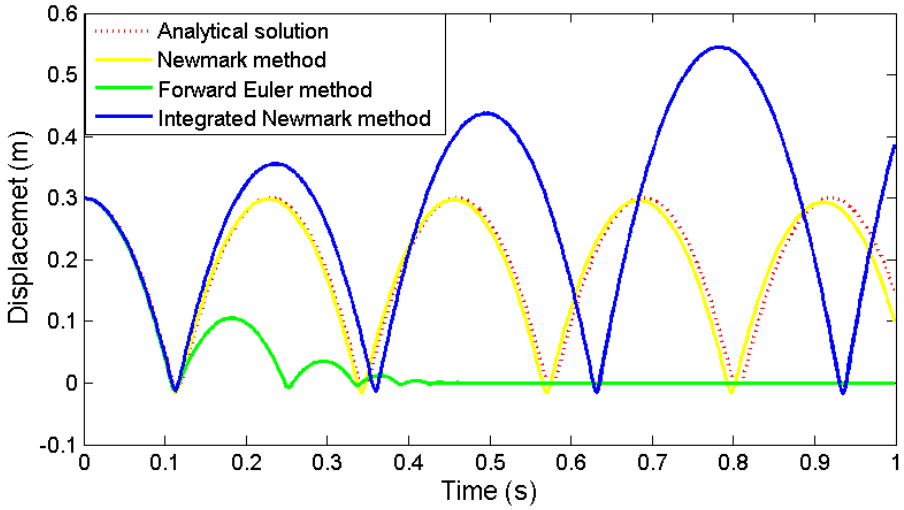

Figure 5.7: Comparison of displacement between the Newmark method, the forward Euler method and the analytical solution in the impacting model. With a time-step size 0.002(s), the forward Eular method shows strong damping effects; the classic Newmark method illustrates a good match with analytical solution; and the integrated Newmark method has an amplifed effects.

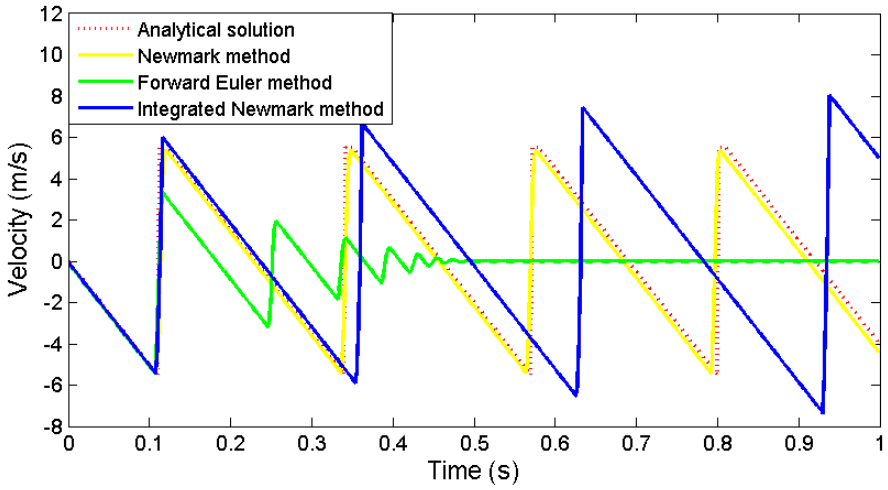

Figure 5.8: Comparison of velocity between the Newmark method, forward Euler method and analytical solution in the impacting model.

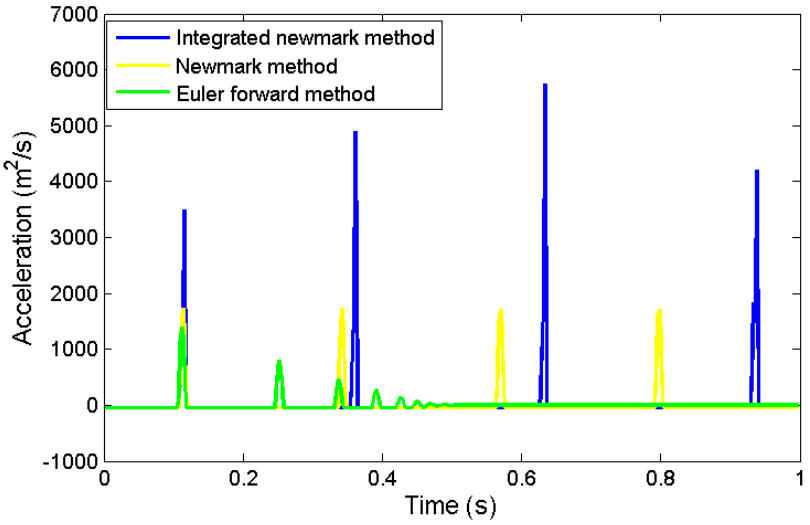

Figure 5.9: Comparison of acceleration between the Newmark method and forward Euler method in the impacting model.

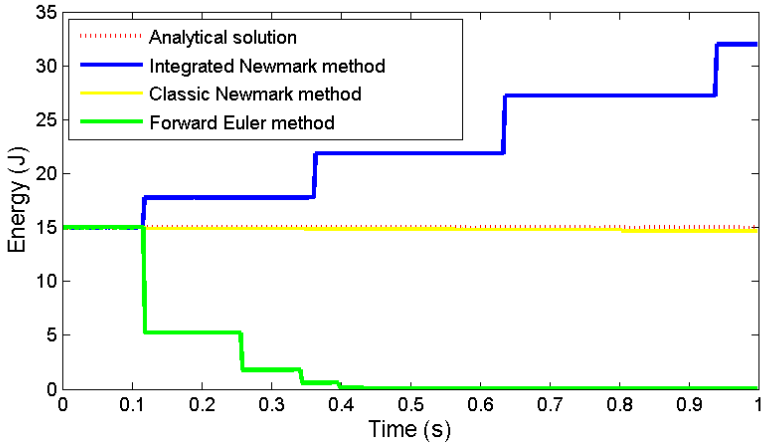

Figure 5.10: Comparison of energy between the Newmark method and forward Euler method in the impacting model.

but when time-step size turns too big – 0.004s – the Newmark solution becomes not stable any more. We can also notice that the Newmark method solution with 0.0025s time-step fits analytical solution better then that of 0.0015s, and this is because of round-off error.

To illustrate the relative error and time-step size relationship more clearly, we define the relative error for impacting model as:

$$E_r = \frac{\sum D_s}{\sum D_a} \tag{5.4}$$

The Figure 5.14 shows relative error and time-step size relationship. The relative error of Euler solution decrease steadily with time-step size, while for the Newmark solution, the relative error decrease very fast and then it stays in a relative stable range (10%) when time-step size less than 0.0025 second. Generally speaking, the error from Newmark simulation is much smaller than that from forward Euler simulation. The relative error of energy in the Newmark method also shows the same trends in comparison with that in the forward Euler method, as Figure 5.15 shows.

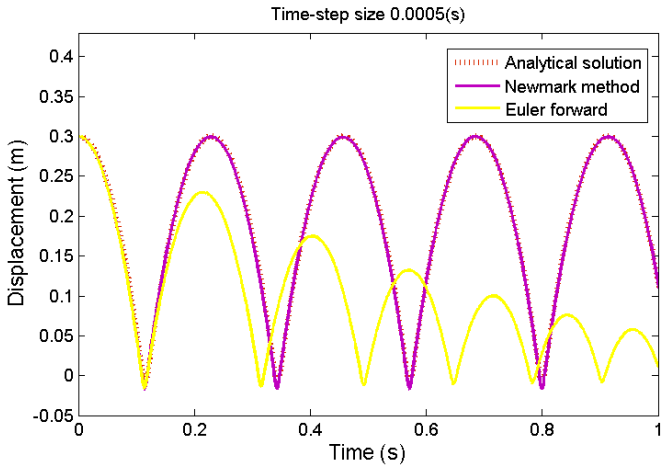

Figure 5.11: Comparison of displacement from the Newmark method, the forward Euler method and the analytical solution in impacting model with time-step 0.0005(s).

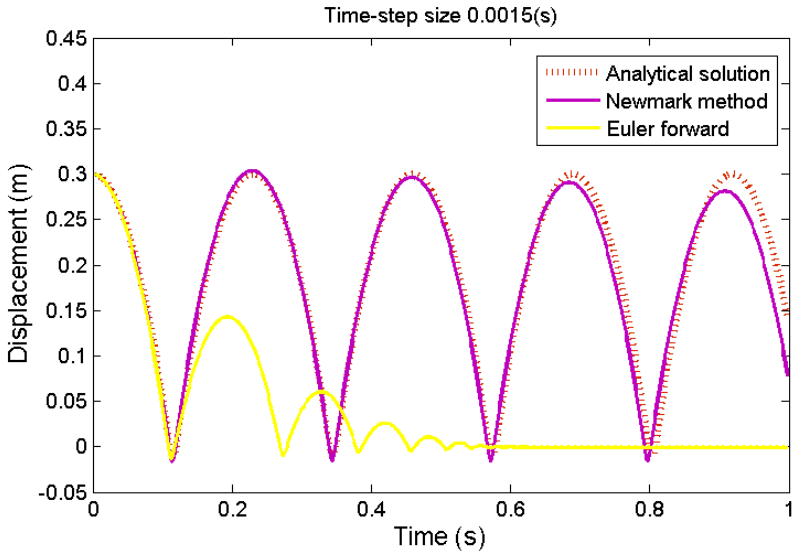

Figure 5.12: Comparison of displacement from the Newmark method, the forward Euler method and the analytical solution in impacting model whose time-step equals to 0.0015(s).

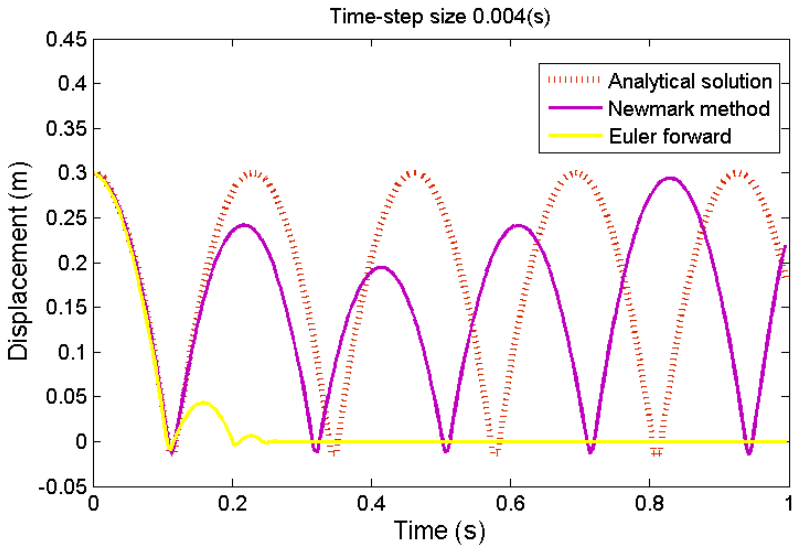

Figure 5.13: Comparison of displacement from the Newmark method, the forward Euler method and the analytical solution in impacting model whose time-step equals to 0.004(s).

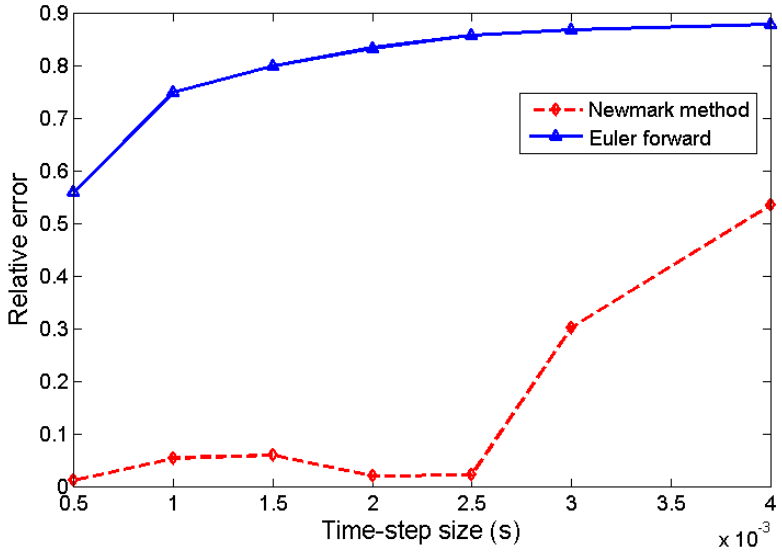

Figure 5.14: The relationship between Relative error and time-step in impacting model using Newmark method and forward Euler method.

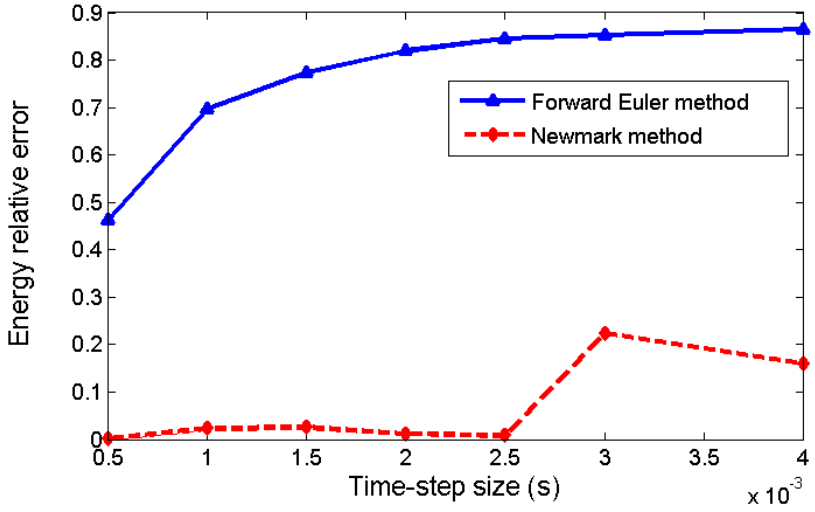

Figure 5.15: The relationship between energy relative error and time-step in impacting model using Newmark method and forward Euler method.

5.3 Summary

The results analysis of the sliding model and the impacting model suggest that the classic Newmark method significantly restricts the damping affects and improves the accuracy, while computational costs remain in the same level. Considering the velocity is the first order derivative of displacement and acceleration is the second order derivative, then the forward Euler method is a first order approximation, and the Newmark method can be considered as a second order approximation. For the impacting process, the change of moving direction results in a sudden change of much higher value of acceleration than average acceleration, and in this situation the second order approximation is able to provide a much better solution than the first order one. For the sliding model, two time-integration method have a similar accuracy as the acceleration keeps the same in the entire process.

Chapter 6

Conclusion and Future Work

We investigated two time integration methods: the forward Euler method and the Newmark method applied to the DDA. Prior to this work, only the forward Euler method was used as a time integration method in the DDA. The forward Euler method is a very stable method, but it leads to severe damping effects in contacting simulation, which is against the corresponding theoretical solution. The major contribution of this work is to derive the Newmark method and apply it to the DDA. The Newmark method avoids the damping effects resulted from time integration simulation. Our work also shows a complete three dimensional DDA simulation, which is rare so far as we know.

It has been an open question for some time whether the damping effect in DDA is an inner defect. With the impacting model, we can see that the damping effects will shrinkage with time-step size, which indicates that when the time-step is small enough, the error resulted from the damping effects can be ignored. But that will cost a high computational time. On the other hand, the Newmark

method keeps the damping effect relatively low when time-step size is reasonable.

In this thesis, for theoretical part, we derived the formula and applied the Newmark method to the DDA. We also developed an integrated Newmark method, in which no velocity and acceleration were included when solving the linear equilibrium equation. But the integrated method is more complicated in practice, and the simulation results show amplifying effects.

For the simulation part, two very basic and very widely used models are applied to test the forward Euler method and the Newmark method. The first one is a sliding model, both the forward Euler method and the Newmark method show a good match with analytical results. The second model is an impacting model, in which the Newmark method shows a much better accuracy than the forward Euler method, and there are barely damping effects.

In future work, more simulations under boarder range of situations are needed to understand how the Newmark method in the DDA works. Also more work could be done to explore Newmark parameters γ, β. We tried to use some different combination of γ, β, but because of the limite of time, the data is not sufficient for meaningful conclusion can be drawn so far. We expect the introduction of the Newmark method improves the accuracy of the DDA and be more widely used in more complected simulations

Bibliography

[1] Y. Liu, *Discrete element methods for asphalt concrete: development and application of user-defined microstructural models and a viscoelastic micromechanical model*. Michigan Technological University, 2011.

[2] M. MacLaughlin and D. Doolin, "Review of validation of the discontinuous deformation analysis (dda) method," *International journal for numerical and analytical methods in geomechanics*, vol. 30, no. 4, pp. 271–305, 2006.

[3] Y. Hatzor and D. Bakun-Mazor, "Modelling dynamic deformation in natural rock slopes and underground openings with dda: review of recent results," *Geomechanics and Geoengineering*, vol. 6, no. 4, pp. 283–292, 2011.

[4] D. M. Doolin and N. Sitar, "Displacement accuracy of discontinuous deformation analysis method applied to sliding block," *Journal of engineering mechanics*, vol. 128, no. 11, pp. 1158–1168, 2002.

[5] A. Hrennikoff, "Solution of problems of elasticity by the framework method," *Journal of applied mechanics*, vol. 8, no. 4, pp. 169–175, 1941.

[6] K. Feng, "Difference schemes for hamiltonian formalism and symplectic geometry," *Journal of Computational Mathematics*, vol. 4, no. 3, pp. 279–289, 1986.

[7] P. A. Cundall and O. D. Strack, "A discrete numerical model for granular assemblies," *Geotechnique*, vol. 29, no. 1, pp. 47–65, 1979.

[8] G.-h. Shi, *Discontinuous deformation analysis: a new numerical model for the statics and dynamics of block systems*. PhD thesis, University of California, Berkeley, 1988.

[9] N. Shimizu, H. Kakihara, H. Terato, K. Nakagawa, *et al.*, "A back analysis method for predicting deformational behavior of discontinuous rock mass," in *2nd North American Rock Mechanics Symposium*, American Rock Mechanics Association, 1996.

[10] T.-C. Ke and J. Bray, "Modeling of particulate media using discontinuous deformation analysis," *Journal of engineering mechanics*, vol. 121, no. 11, pp. 1234–1243, 1995.

[11] Y. Ohnishi, G. Chen, and S. Miki, "Recent development of dda in rock mechanics," *Proc. ICADD*, vol. 1, pp. 26–47, 1995.

[12] G.-h. Shi *et al.*, "Three dimensional discontinuous deformation analyses," in *DC Rocks 2001 The 38th US Symposium on Rock Mechanics (USRMS)*, American Rock Mechanics Association, 2001.

[13] T. Ke, "Improved modeling of rock bolting in dda," in *Proc., 9th Int. Conf. on Computer Methods and Advances in Geomechanics*, pp. 483–488, Balkema, Rotterdam, The Netherlands, 1997.

[14] M. Yeung, Q. Jiang, and N. Sun, "Validation of block theory and three-dimensional discontinuous deformation analysis as wedge stability analysis methods," *International Journal of Rock Mechanics and Mining Sciences*, vol. 40, no. 2, pp. 265–275, 2003.

[15] K. Shyu, X. Wang, and C. Chang, "Dynamic behaviors in discontinuous elastic media using dda," in *Proceedings of the Third International Conference on Analysis of Discontinuous Deformation from Theory to Practice*, pp. 243–252, 1999.

[16] X. Dong, A. Wu, and F. Ren, "A preliminary application of discontinuous deformation analysis (dda) to the three gorges project on yangtze river, china," in *Proceedings of the first international forum on discontinuous deformation analysis (DDA) and simulations of discontinuous media, Berkeley, USA*, pp. 310–317, 1996.

[17] H. K. Law and I. P. Lam, "Evaluation of seismic performance for tunnel retrofit project," *Journal of geotechnical and geoenvironmental engineering*, vol. 129, no. 7, pp. 575–589, 2003.

[18] Y. Hatzor *et al.*, "Dynamic rock slope stability analysis at masada national monument using block theory and dda," *Rock Mecganics for Industry*, vol. 1, pp. 63–70, 1999.

[19] J. Kottenstette, "Dda analysis of the rcc modification for pueblo dam," in *Proceedings of Third International Conference on Analysis of Discontinuous Deformation-From Theory To Practice, Vail, Co, Jun*, pp. 3–4, 1999.

[20] Q. Jiang, Y. Chen, C. Zhou, and M.-c. R. Yeung, "Kinetic energy dissipation and convergence criterion of discontinuous deformations analysis (dda) for geotechnical engineering," *Rock mechanics and rock engineering*, vol. 46, no. 6, pp. 1443–1460, 2013.

[21] D. M. Doolin and N. Sitar, "Time integration in discontinuous deformation analysis," *Journal of engineering mechanics*, vol. 130, no. 3, pp. 249–258, 2004.

[22] M. Tsesarsky, Y. Hatzor, and N. Sitar, "Dynamic block displacement prediction–validation of dda using analytical solutions and shaking table experiments," in *Stability of rock structures: Proceedings of the Fifth International Conference of Analysis of Discontinuous Deformation. Lisse: Balkema Publishers*, pp. 195–203, 2002.

[23] A. R. Keneti, A. Jafari, and J.-H. Wu, "A new algorithm to identify contact patterns between convex blocks for three-dimensional discontinuous deformation analysis," *Computers and Geotechnics*, vol. 35, no. 5, pp. 746–759, 2008.

[24] J. Liu, Z. Nan, and P. Yi, "Validation and application of three-dimensional discontinuous deformation analysis with tetrahedron finite element meshed block," *Acta Mechanica Sinica*, vol. 28, no. 6, pp. 1602–1616, 2012.

[25] R. Grayeli and K. Hatami, "Implementation of the finite element method in the three-dimensional discontinuous deformation analysis (3d-dda)," *International journal for numerical and analytical methods in geomechanics*, vol. 32, no. 15, pp. 1883–1902, 2008.

[26] M. S. Khan, *Investigation of discontinuous deformation analysis for application in jointed rock masses*. PhD thesis, University of Toronto, 2010.

[27] M.-c. R. Yeung, *Application of Shi's discontinuous deformation analysis to the study of rock behavior*. PhD thesis, University of California, Berkeley, 1991.

[28] M. MacLaughlin and N. Sitar, "A gravity turn-on routine for dda," in *ICADD-3 Third International Conference on Analysis of Discontinuous Deformation from Theory to Practice. American Rock Mechanics Association*, pp. 65–73, 1999.

[29] M. M. MacLaughlin, *Discontinuous deformation analysis of the kinematics of landslides*. PhD thesis, University of California, Berkeley, 1997.

[30] J. Lin, R. Al-Zahrani, A. Munjiza, and D. Lee, "Large displacement and finite strain dda: an implementation and physical verification," in *Proceedings of the Second International Conference on Analysis of Discontinuous Deformation, Kyoto, 10-12 July*, pp. 245–252, 1997.

[31] M. MacLaughlin, N. Sitar, D. Doolin, and T. Abbot, "Investigation of slope-stability kinematics using discontinuous deformation analysis," *International Journal of Rock Mechanics and Mining Sciences*, vol. 38, no. 5, pp. 753–762, 2001.

[32] M. M. MacLaughlin, N. Sitar, *et al.*, "Kinematics of sliding on a hinged failure surface," in *2nd North American Rock Mechanics Symposium*, American Rock Mechanics Association, 1996.

[33] T. Ke, "Application of dda to simulate fracture propagation in solid," in *Proceedings of the Second International Conference on Analysis of Discontinuous Deformation*, pp. 155–185, Japan Institute of Systems Research: Kyoto, Japan, 1997.

[34] T. J. Hughes, R. L. Taylor, J. L. Sackman, A. Curnier, and W. Kanoknukulchai, "A finite element method for a class of contact-impact problems," *Computer Methods in Applied Mechanics and Engineering*, vol. 8, no. 3, pp. 249–276, 1976.

[35] N. M. Newmark, "A method of computation for structural dynamics," in *Proc. ASCE*, vol. 85, pp. 67–94, 1959.

[36] H. M. Hilber, T. J. Hughes, and R. L. Taylor, "Improved numerical dissipation for time integration algorithms in structural dynamics," *Earthquake Engineering & Structural Dynamics*, vol. 5, no. 3, pp. 283–292, 1977.

[37] S. Krenk, "Energy conservation in newmark based time integration algorithms," *Computer methods in applied mechanics and engineering*, vol. 195, no. 44, pp. 6110–6124, 2006.